Charles University
Faculty of Science

Study program: Biology

Branch of study: Immunology

Bc. Petra Hadlová

Cytometric assay of antigen-specific T cell response in monitoring of BCG vaccine therapy

Cytometrický test antigen-specifické T buněčné odpovědi pro monitoring terapií BCG vakcínou

Diploma thesis / Diplomová práce

Supervisor: RNDr. Karel Drbal, Ph.D.

Praha 2019

Prohlášení

Prohlašuji, že jsem závěrečnou práci zpracovala samostatně a že jsem uvedla všechny použité informační zdroje a literaturu. Tato práce ani její podstatná část nebyla předložena k získání jiného nebo stejného akademického titulu.

V Praze dne 3. 1. 2019

.....

Petra Hadlová

Poděkování

Předně bych ráda poděkovala svému školiteli RNDr. Karlu Drbalovi, Ph.D. za jeho odbornou pomoc, rady a trpělivost při vedení mé diplomové práce. Dále bych ráda poděkovala doc. MUDr. Tomáši Kalinovi za poskytnutí CMV lyzátu, příslušných reagencií a metodiky. Prof. Michaelu Bachmannovi děkuji za příležitost k načerpání zkušeností v jeho laboratoři na praktické stáži. Na závěr bych ráda poděkovala své rodině obzvlášť svým rodičům a sestře za jejich podporu, pomoc a trpělivost během celého studia.

Abstract

Bladder carcinoma (BCa) is among the most common carcinomas in the Western world. Despite the availability of effective therapies, there is currently an urgent need to develop a stratification method, which would enable the accurate identification of patients responsive to therapy. In the theoretical part of my diploma project I describe the heterogeneity of BCa and the currently applied immunotherapeutic approaches. I specifically focused on the *Bacillus Calmette-Guérin* (BCG) vaccine instillation. For decades another use of BCG has been a prophylactic vaccination against tuberculosis (TB) infection. BCG serves as a model treatment because it is highly efficient when prescribed to the responsive patient. However, an effective stratification is yet to be developed for BCa and latent tuberculosis infection (LTBI) diagnosis and/or monitoring.

In the experimental part of my project, I developed and tested a 10-parameter panel for T cell-specific activation test (TAT) applicable for a stratification of BCa patients as well as for the detection of LTBI. I tested the panel on positive controls using flow cytometry (FCM) method because it allows for detection and measurement of dozens of markers at a single cell level. It is easily applicable to available urine and blood samples obtained from BCa patients.

Combination of TAT markers allowed me to detect reactive T cell population after polyclonal and antigen-specific stimulation. Therefore, I conclude that the TAT panel is suitable for further development and validation of a patient stratification method based on the detection of antigen-specific T cell response.

Key words: T-cell response, flow cytometry, *in vitro* activation test, tumor immunotherapy, patient stratification, personalized medicine

Abstrakt

Karcinom močového měchýře patří mezi nejčastější karcinomy v západním světě. Navzdory dlouhodobému výzkumu a existenci efektivních terapeutických možností přetrvává potřeba vyvinout stratifikační metodu, která umožní identifikovat pacienty odpovídající na léčbu. V teoretické části své diplomové práce jsem popsala heterogenitu karcinomu močového měchýře, jako modelové patologie a terapeutické přístupy, které se v současnosti uplatňují. Obzvlášť jsem se soustředila na terapii založenou na instilaci *Bacillus Calmette-Guérin* (BCG). BCG je po desetiletí používaná jak při léčbě karcinomu močového měchýře, tak jako preventivní vakcína proti infekční tuberkulóze (TB). BCG slouží jako modelová terapie, protože u odpovídajících pacientů je vysoce účinná. Nicméně, pro zlepšení diagnostiky a monitorování průběhu onemocnění karcinomu močového měchýře a latentní tuberkulózy (LTBI) chybí účinná stratifikační metoda.

V experimentální části své práce jsem navrhla a testovala 10 parametrický panel pro detekci T buněčné odpovědi na aktivaci (TAT) pro budoucí využití při stratifikaci pacientů s nádorem močového měchýře a pro detekci (LTBI). Panel jsem testovala na pozitivních kontrolách metodou průtokové cytometrie, která umožňuje detegovat desítky znaků na jednotlivých buňkách. Je dobře využitelná pro zpracování a měření snadno dostupných pacientských vzorků moči a krve.

Kombinace znaků zahrnutá v TAT panelu mi umožnila detegovat reaktivní T buněčné populace po polyklonální a antigen-specifické stimulaci. Došla jsem proto k závěru, že mnou vytvořený panel je vhodný pro další rozvíjení stratifikační metody na základě detekce antigen specifické T buněčné odpovědi.

Klíčová slova: T-buněčná odpověď, průtoková cytometrie, aktivační test *in vitro*, imunoterapie nádorů, stratifikace pacientů, personalizovaná medicína

Contents

List of the abbreviations used in the thesis

Ab	antibody
Ag	antigen
APC	antigen presenting cell
BCa	bladder carcinoma
BCG	Bacillus Calmette-Guérin
EMA	European Medicines Agency
FCM	flow cytometry
FDA	Food and Drug Administration
LPS	lipopolysaccharides
mAb	monoclonal antibody
MHC	major histocompatibility complex
MIBC	muscle invasive bladder carcinoma
NMIBC	non-muscle invasive bladder carcinoma
PBMC	peripheral blood mononuclear cells
PHA	phytohemagglutinin
PMA	phorbol 12-myristate, 13-acetate
scFv	single chain variable fragment
TAT	T cell activation test
TM	target module
TSA	tumor-specific antigen
TST	tuberculin skin test
TURB	transurethral resection of bladder
uniCAR	universal chimeric antigen receptor T cell

1. Introduction

Bladder carcinoma (BCa) is among the most common carcinomas in the Western world with high recurrence rates. Patients are treated using numerous therapies including transurethral resections of the bladder (TURB), chemotherapy and immunotherapies such as BCG vaccine instillation and recently also checkpoint inhibition. However, the routinely applied monitoring tests are still falling short in terms of accurate stratification of responsive patients to the individual treatment options.

For the above stated reasons, I decided to work on designing an efficient stratification method, with a particular focus on BCG-based treatment. BCG vaccine is a vaccine from attenuated *M. bovis* strains and alongside the BCa treatment it has been historically used to vaccinate patients against tuberculosis infection (TB).

Therefore, my first goal was to design a T cell activation test (TAT) panel, which incorporated the knowledge of previous studies on detection of active TB and latent tuberculosis infection (LTBI). To detect the expression of the included markers, I chose the method of flow cytometry (FCM). FCM is optimal for detection of multiple markers in one assay allowing to identify rare antigen-reactive T cell populations and describe their phenotype in detail.

Using the designed TAT panel my next goal was to optimize positive controls (polyclonal stimuli PHA lectin and PMA/ionomycin) for the future use of TAT in BCa and LTBI patient stratification and monitoring. Then I decided to test the capability of TAT to detect antigen-specific T cell response using CMV lysate in order to confirm its efficiency to detect rare populations. Lastly, I wanted to exploit the uniCAR T cell system as another form of antigen-specific control

2. Theoretical background

2.1. Heterogeneity of bladder carcinoma

In Czechia, bladder carcinoma (BCa) is the sixth most common carcinoma in men and the eleventh in women. The incidence is the highest for patients between 60 and 80 years of age[1]. The overall 5-year survival rate reaches 70%[2]. Even though the survival rate is highly promising there is a lot of potential for improvement. Despite the use of effective treatment options, including BCG immunotherapy established since 1975[3], the recurrence rate of high-risk BCa reaches 39.1%. Additionally, 33.1% of patients progress within 10 years[4]. To decrease the incidence of recurrence and progression it is essential to develop an efficient stratification method, which will improve the diagnosis and monitoring of the progress of treatment.

Based on tumor, node, metastasis (TNM) classification, BCa is divided into non-muscle invasive bladder carcinoma (NMIBC) and muscle invasive bladder carcinoma (MIBC), which can progress to metastatic state[5]. The NMIBC represents 70% of all BCa[6]. WHO introduced the first grading system in 1973, updated it in 2004 and in 2016. Based on the new grading system, NMIBC covers a spectrum of papillary carcinomas divided into three major categories, neoplasms of low malignant potential, low-grade (LG) and high-grade (HG) carcinoma[7]. Regarding staging, NMIBC, a superficial type of the disease, covers Ta, T1 and flat carcinoma in situ (CIS) lesions[5] based on TNM staging. The MIBC covers the stages T2-T4b and is characterized by a high potential of developing metastases, which significantly worsens patient's prognosis[5].

The European Association of Urology (EAU) guidelines set a standard of care for BCa based on risk stratification. BCa tumors are divided into low-, intermediate- and high-risk ones[8]. The risk is evaluated based on the progression probability of a tumor from the non-muscle invasive to the muscle invasive stage[9].

Transurethral resection of bladder tumor (TURB) is a first-line treatment for the intermediate and high-risk tumors. TURB is followed by re-TURB and a single-shot chemotherapy and an instillation of BCG[10]. In case the BCG instillation fails or is not well

tolerated by the patient, the EAU guidelines recommend application of intravesical chemotherapy with cisplatin or mitomycin C as part of the bladder-preserving strategy. In case the chemotherapy fails and further progression is detected, EAU guidelines suggest to opt for radical cystectomy in order to stop the progression of the disease[11].

The standard treatment for MIBC is radical cystectomy combined with neoadjuvant chemotherapy and neoadjuvant/adjuvant radiotherapy. Adjuvant therapy is an additional therapy prescribed in order to decrease the size of tumor before the target therapy or therapy following the initial surgery to achieve remission[5].

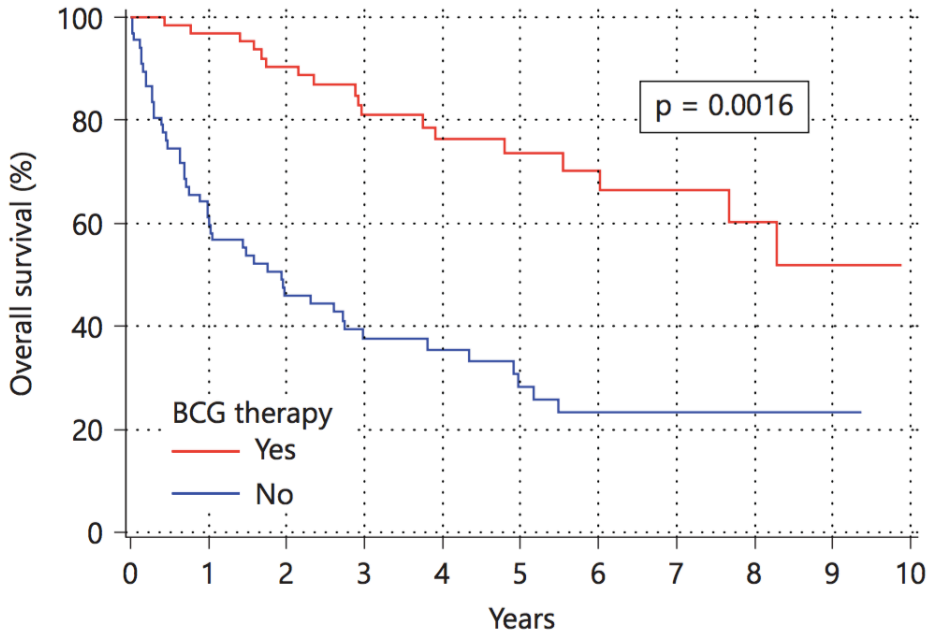

Figure 1. Comparison of survival of high grade (HG) BCa patients treated with BCG instillation therapy with those not treated with BCG. *Red curve represents patients who received the BCG therapy. Blue curve represents patients not treated by BCG therapy. The survival was documented for ten years. The effects of BCG therapy leads to 5-year survival in 74% of patients compared to 28% in patients with no BCG therapy and twice as many patients reaching 10-year survival* [12].

Of all the treatment options, BCG immunotherapy prescribed to responsive patients is

currently the major option leading to long-term clearance of the high-risk tumor and around 30% higher disease-free survival as illustrated in *Figure 1.*

2.2. BCa Immunotherapy

There are currently several available options to treat BCa exploiting the power of individual patient's immune system.

Innate immune system is crucial for the eradication of the incoming pathogens entering the body and their clearance. Additionally, it works as a mediator and an initiator of the adaptive immune response, playing an essential role in tumor surveillance and eradication. Innate immune system operates on cellular (NK cells, dendritic cells, macrophages and mast cells) and humoral (complement, cytokines) levels.

Adaptive immune system works in an antigen-specific manner and leads to highly precise eradication of the tumor cells. T cells, which recognize the newly arising tumor-specific neoantigens can specifically and effectively target the clonal tumor cells, expressing the neoantigens[12]. It has been shown that non-coding regions are a particularly rich source of tumor-specific neoantigens, allowing cytotoxic $CD8^+$ T cells to target the tumor. The great advantage of the use of such antigens is that they can be shared among patients, which allows for a broader group of patients to benefit from them[13].

2.2.1. BCG treatment

BCG vaccine employs both arms of the immune system in the process of BCa eradication and TB prevention. The vaccine consists of attenuated live strains of *Mycobacterium bovis*. *M. bovis* is routinely employed for high-risk patients in two areas of disease treatment. The first one is BCa. The stratification of patients for BCG immunotherapy must determine whether the patient has a reactive T cell clone against antigens specific to the administered *M. bovis* and whether they will mount the immune response against the tumor-antigens in order to prescribe the therapy to responsive patients.

The second field is the prophylactic use of *M. bovis* against a similar microorganism (*M. tuberculosis*). The prophylaxis works in the form of a vaccine against tuberculosis infection (TB) with *M.tuberculosis*. The protective treatment functions on the basis of antigenic mimicry between M. *bovis* and tumor-specific neoantigens in case of BCa and *M. bovis* and *M. tuberculosis* in case of TB[14].

2.2.1.1. BCG vaccine instillation

BCG is applied as a first line modality for early intermediate- and high-risk NMIBC BCa patients in the form of lyophilized vaccine instillation[15]. Several strains have been used for BCa treatment including, Tice, Montreal, Pasteur, Connaught and Connaught and Tice. It has been demonstrated that the individual strains partially differ in their therapeutic efficacy[16]. Its functionality stems from the effect of bacterial infection on the tumor cells and by inducing the host's immune response.

The instillation schedule and the dose of the BCG vaccine are a highly discussed topic. Currently EAU guidelines suggest instillation series spanning three years starting with 6x weekly at 0 month and then following 3x weekly at 3, 6, 12, 18, 24, 36 month[11].

Immune response to the BCG therapy can be divided into three main phases. The initial one is infection of the bladder cells followed by the induction of immune response which leads to the development of antitumor response[6,17]. The BCG mechanism has been coherently depicted in a review by Redelman *et al*., and is presented in *Figure 2*[17].

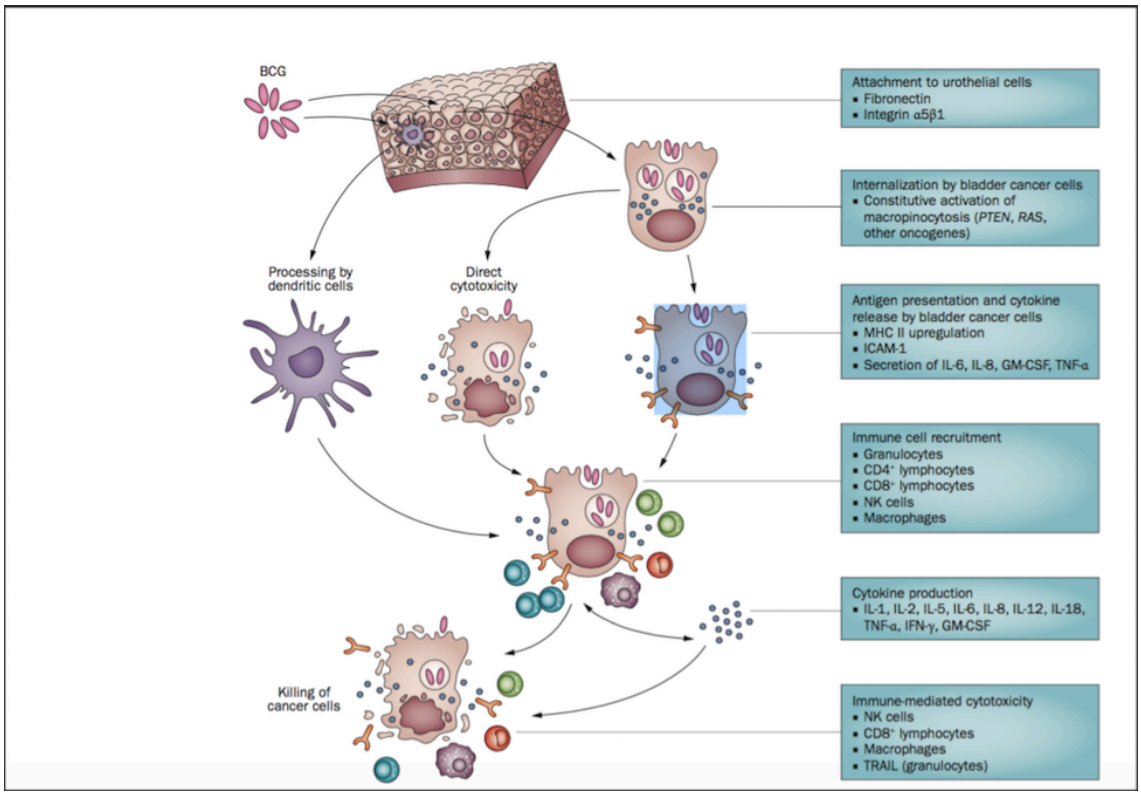

Figure 2. Mechanism of BCG vaccine treatment*. The scheme depicts the mechanism behind BCG vaccine effect. After its application, the vaccine is absorbed through macropinocytosis, employs MHCII molecules mechanism and presents the antigens to the immune cells. Adaptive immune cells, both $CD4^+$ and $CD8^+$ T cells are recruited and through cytokine release and the immediate cytotoxicity destroy the tumor cells*[17].

First, the BCG is attached through the fibronectin, which leads to its absorption via macropinocytosis by the BCa cells[18,19]. Upon the instillation, the BCG vaccine induces release of antimicrobial peptides, such as β-defensins and cathelicidins, which are induced by the activation of mitogen activated protein kinase (MAPK) signalling pathway. MAPK signalling pathway carries signal from the surface of the cell to the nucleus of the cell via series of phosphorylative reactions and results in protein synthesis. MAPK signalling pathway has also been tested as a potential target of BCa treatment. It has been found that p38 MAPK inhibition resulted in decrease of proliferation rate in BCa cell lines including RT112, T24 and UM-UC-3 routinely used in research[20].

Another important mechanism of the innate immune response, which has been researched for its predictive properties is degranulation[21]. Degranulation belongs among the earliest detectable signs of immune system activation.

The most important innate immune cells for BCG vaccine efficiency are natural killer (NK) cells. NK cells are activated through NKG2D receptor and produce IFNγ which leads to induction of M1 macrophages. Increased numbers of M1 macrophages have been detected in regressing BCa tumors[22]. The NK cells also lead to eradication of tumor cells by perforin release, which results in membrane disruption of the effected tumor cell through perforin-granzyme pathway[23]. Increased numbers of NK cells were detected in NMIBC patients' peripheral blood compared to healthy donors, 13.8% vs 5.56% respectively[24].

Last essential involvement of innate immune response on cellular level are neutrophils. Neutrophils secrete TNF-related apoptosis-inducing ligand (TRAIL. In tumor cells, expression of TRAIL results in apoptosis, which means that neutrophils are directly involved in eradication of the tumor[15].

The BCG treatment leads to induction of adaptive immune response, more precisely systemic, Th1 effector response, tolerization, Th2 response or regulatory Th17 response. The polarization between the two depends on released cytokines. Th1 cells produce IL-2, IFNγ and TNFβ while Th2 produce IL-4, IL-5, IL-10 and IL-13[25]. BCG is a Th1 polarizing therapy. Th1 induction is crucial for the effectiveness of BCG therapy in BCa patients[26,27]. The induction of adaptive immune response was proved in research, when cytokines including IL-1β, IL-10 and TNF-α were detected 24 hours after the BCG instillation at 1st and 6th week.

However, Th1 response is also the main disadvantage of the therapy. If the BCG therapy is not tolerated well by the patient it can lead to serious systemic side effects[26,28–30]. Therefore, the instillation schedule and the dose of the BCG vaccine remain a discussed topic. The goal is to maximize the efficiency and minimize adverse side effects.

2.2.1.2. BCG vaccine against TB infection

BCG has been used as a prophylactic vaccine against TB since 1921[31]. It has proved effective yet it still fails to completely prevent lung TB[32]. In 2009 WHO issued a TB warning on the basis of high number of people suspected of carrying the latent TB infection (LTBI). Based on WHO issued guidelines, active TB infection is a state when

M. tuberculosis, cause of TB disease starts multiplying in the infected individual and manifests symptoms including cough lasting longer than 3 weeks. In contrast to active TB infection, LTBI is not clinically symptomatic but bears the risk of developing into the active form at any time. Currently 25% of the world's population are estimated to be at risk of carrying LTBI[32]. Despite that, vaccination programs in developed countries (incl. Czechia) decreased. Currently only children from high-risk groups based on epidemiology findings are subjected to vaccination. Non-vaccinated children are considered at risk of developing LTBI if exposed to active TB infection in their household[33]. Lack of vaccination may cause significant problems for the local healthcare systems, especially in places with lower healthcare standards or in cases when patients come to the doctor too late.

The immune response to BCG vaccination is not yet completely understood. The initial interaction between BCG antigens and the immune system occurs on the level of innate immune response, more specifically macrophages. The interaction occurs via pattern recognition receptors (PRR), namely TLR2/4 and complement receptor 3[32].

BCG also interacts with dendritic cells (DC), which present the BCG-specific antigens to naïve T cells in lymph nodes through the DC-SIGN receptor. Additionally, *in vitro* DC increase their antigen presenting properties upon BCG presentation. The last major component of innate immunity, which is crucial for the establishment of memory against BCG are neutrophils[32].

To create a long-term memory B cells are highly significant. B cells participate in the opsonisation process in the initial stages of infection, which allow for phagocytosis by the cells of innate immunity and result in the antigen presentation to T cells[32]. Upon the interaction with BCG, neutrophils release a number of cytokines and induce Th1 and Th17 cells, which play an essential role in controlling TB[34]. The role of $CD4^+$ T cells in TB immunity has been described in more detail than $CD8^+$ T cells especially for their role in establishing central memory and for production of IFNγ (essential for resistance against *M. tuberculosis* infection)[35].

Clear overlap between the effects of *M. bovis* and *M. tuberculosis* was recently proved even in BCa therapy when live attenuated *M. tuberculosis* vaccine, MTBVAC was used to treat a mice model of BCa. The tests showed promising results, with only <10%

mortality in treated mice. One of the main advantages of MTBVAC application over the routinely used BCG MEDAC vaccine instillation is the possibility to accurately identify and describe the applied strain[18].

2.2.2. Checkpoint inhibitors

BCa is a suitable pathology for another form of immunotherapy, checkpoint inhibition therapy because of its high mutational burden. At 8.03 mutations per megabase (Mb), it is among tumors with the highest mutational burden in adults[36]. High number of mutations significantly increases the statistical probability of an expression of tumor-specific antigen and the existence of corresponding antigen-reactive T cell clone.

The checkpoint inhibitors unblock the adaptive immune system and in effect lead to activation of tumor-specific cytotoxic T cells[12]. The checkpoint inhibitors are primarily prescribed to MIBC patients. The overview of basic mechanism of checkpoint inhibition is shown in *Figure 3*. $CD8^+$ T cells target the tumor cells by perforin granzyme pathway[23]. $CD4^+$ T cells have also been proved to play an essential role in tumor immunity both as tumor suppressive cells and as immune regulatory cells[37].

So far several checkpoint inhibitors have been identified and are routinely used in the clinic, PD-1 (PDCD1), PD-L1 (CD274), CTLA-4 (CTLA-4)[38]. Additionally TIM-3 (HAVCR2), LAG-3 (LAG3) and TIGIT (TIGIT) are under investigation for introduction into the clinical practice[39].

Food and drug administration (FDA) agency in the USA approved five checkpoint inhibition drugs to treat BCa specifically, in both first and second line of treatment for unressectable T3-T4 tumors and patients not eligible for cisplatin based therapy[40].

The currently approved checkpoint inhibition immunotherapy for BCa targets PD-1 (PDCD1), (nivolumab, pembrolizumab)[41] and PD-L1 (CD274), (avelumab, durvalumab, atezolizumab)[42] molecules.

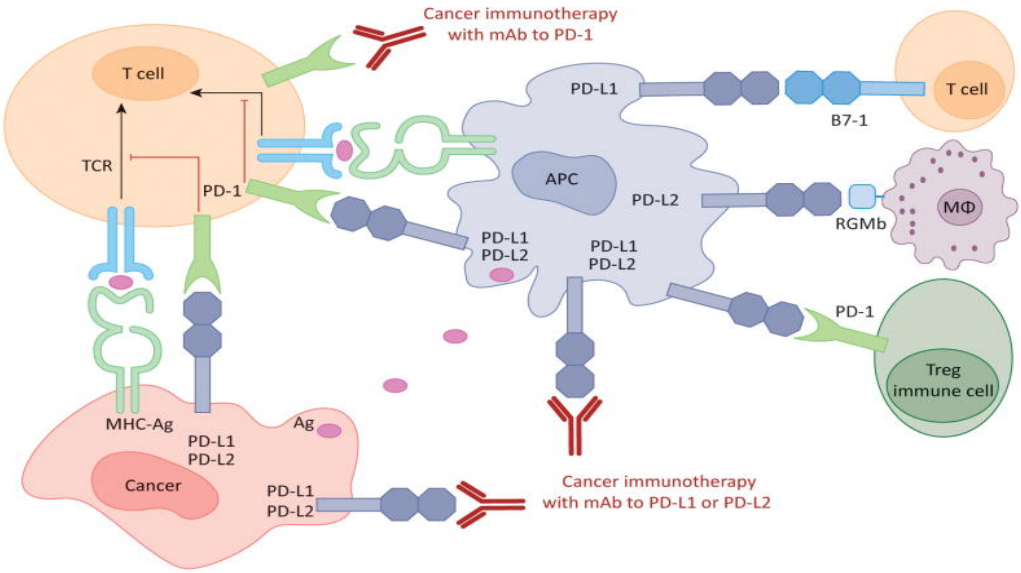

Figure 3. The overview of mechanism of checkpoint inhibitor therapy*. The scheme depicts two major checkpoint inhibitors used for treatment of BCa targeting PD-1 and PD-L1 molecules. Once the checkpoint inhibitors are blocked the T cells become effective. The tumor-antigen specific T cells target tumor cells. This results in a clearance of the tumor*[46].

Following the FDA approval, EU authority European Medicines Agency (EMA) approved nivolumab, pembrolizumab and atezolizumab for BCa treatment in 2017 and in Czechia. A major disadvantage in Czechia is that the application of the drugs to patients is not yet covered by the regular health insurance and therefore, can only be administered to patients participating in a clinical study.

This led me to choose the stratification of patients with the potential to receive BCG, as the only routinely available and applied immunotherapy for BCa. However, the knowledge will be applicable to other forms of immunotherapy.

2.2.3. Adoptive cell therapy – uniCAR T cells

Another possibility, which is not routinely applied in the treatment of tumors is a type of cell therapy, specifically chimeric receptor (CAR) T cells, and more precisely universal chimeric receptor (uniCAR) T cells. So far, the uniCAR therapy has been applied in treatment of liquid tumors. These are artificially engineered transgenic T cells whose major advantage is that they circumvent the MHC molecule – Ag presentation pathway,

mediating direct interaction between T cell and the tumor cell in the body via an Ag-specific binding construct, see *Figure 4* for a scheme of the construct, bridging tumor and effector T cell.

The uniCAR system combines the intracellular CD28/CD3ζ domain with the binding element designed from the single chain variable fragment (scFv) domain, also referred to as target module (TM), connected by a flexible linker and activating universal immune receptor. Additionally, the construct requires an extracellular hinge, spacer element and endodomain, responsible for signalling via immunoreceptor tyrosine activation motif (ITAM).

UniCAR T cell system allows the TM to be interchangeable[43]. TM may be designed to bind to diverse tumor-specific antigens. The brilliance of the system is in the target modules, which have an affinity to the target cell and to the T cell and can be easily replaced as a soluble molecule[44,45].

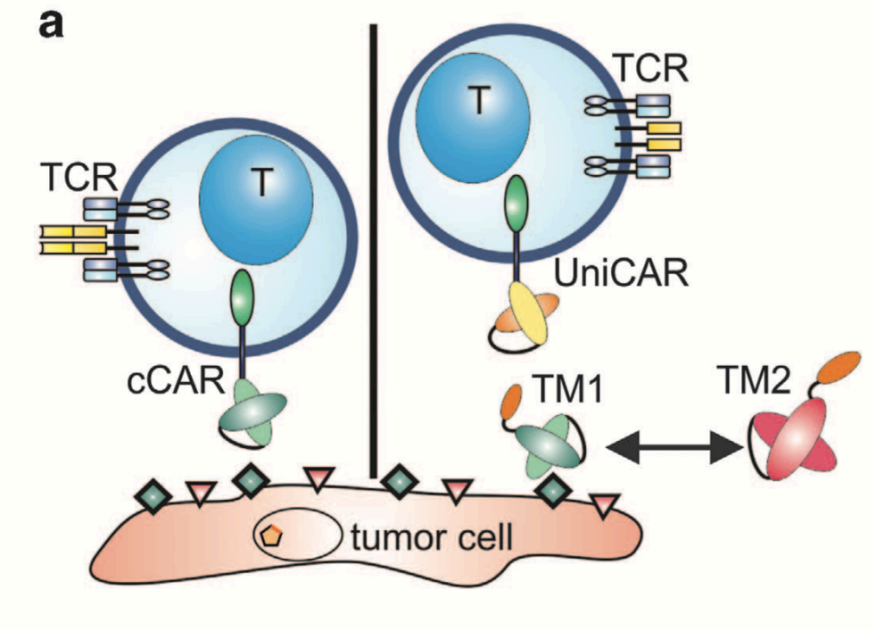

Figure 4. Construction of uniCAR T cells*. The conventional CAR T cells (here labeled cCAR) contain scFv fragment, which determines the affinity of the construct to T cell receptor. The scFv is connected to the transmembrane domain via a hinge. On the other side of the construct signalling domains enable the activation of T cell. The uniCAR consists of two parts. The first one allows manipulation with T cells in a non-stimulatory manner and the second one is a specific TM, which allows for induced activation of TSA specific T cells.*[48]

Recently, novel TM has been developed, which does not recognize a cell surface TSA but rather a short peptide, E5B9 derived from nuclear autoantigen La/SS-B[44] .

2.3. BCa monitoring methods currently used in the clinics

Monitoring of the immune response has been a challenge since the very beginning of the BCG treatment of BCa[3]. A wide scope of methods is available including pathological assessment, identification of molecular biomarkers, monitoring of cell response, detection of local (urinary) and systemic (blood) cytokines and identification of genomic signatures[46]. The monitoring methods could also be divided to local and systemic approaches based on the scale of the detected markers.

2.3.1. Cytology

Routine monitoring on the local scale includes cytology of samples biopsied from the bladder. Cytology is based on identification of cells released from the surface of bladder. Relying on cytology for diagnosis and monitoring proved problematic dues to two factors. First major downside is the low sensitivity in cases of low-grade tumors. Second is the high variation in assessment of the samples among pathologists, which led to establishment of the Paris System in 2013[47]. The Paris System provides a unified, standardized terminology and scaling system to allow for more accurate diagnostics and monitoring of BCa[48]. However, the sensitivity of cytology in newly diagnosed patients has been reported as low as 28%[49].

Two more local monitoring methods are currently available in the clinics, BladderChek nuclear matrix protein-22 (NMP-22) and Urovysion Fluorescent in situ hybridization (FISH)[49].

2.3.1. BladderChek and Urovysion FISH

BladderChek NMP-22 detects the presence of NMP-22, which indicates presence of transitional cell carcinoma[50]. Sensitivity of BladderChek MMP2 reaches 88%[49].

Urovysion FISH detects abnormalities in chromosomes 3, 7, 17 and 9p21[51]. Sensitivity of Urovysion FISH reaches 80%. The conclusion from a comparative study of BladderChek

vs Urovysion FISH is to use BladderChek test as it provides the best price-performance ratio and significantly improves the prediction and monitoring of BCa[49]. The FISH method has been used to predict recurrence in patients undergoing BCG therapy and led to promising results. Patients with FISH positive results prior to BCG vaccine instillation, had a 3 to 5 times higher chance of tumor recurrence[52]. This means a FISH method can also be incorporated into a panel of detection and monitoring methods for BCG therapy.

2.3.2. Cytokine detection

In general, there is a high tendency to identify as many markers at once as possible. Markers, which may be detected using non-invasive methods, to spare the patient from undergoing further procedures are preferable. The sample of choice is urine[53,54]. So far IL-2[26] and soluble intercellular adhesion molecule (ICAM-1)[53] have been detected in urine. These cytokines and markers are released in response to T cell specific activation. An entire panel of cytokines present in urine prior to BCG installation, which predicted the recurrence of BCa with 85.5% accuracy has been identified. Prediction cytokines are IL-2, IL-8, IL-6, IL-1ra, IL-10, IL-12[p70], IL-12[p40], TRAIL, and TNF-α[55]. In another study on cytokine release into urine after BCG instillation, IL-17 was added to the panel of previously listed cytokines. The analysis was performed using FCM and led to a conclusion that the response and prediction values are highly personal[56].

Out of the presented list of cytokines, IL-2 and IFNγ have also been used for detection of systemic response[57]. Another study expanded the list of cytokines detectable in both urine and serum to include IL-4, GM-CSF, IFNγ, IP-10, MIP-1a, PDGF, MIP-1b,RANTES and VEGF[54].

The systemic approaches include tests performed on patients' peripheral blood. Cytokine producing cells were detected both prior to and after BCG installation.

2.3.3. Proteome testing

New approaches to monitoring the immune response to BCG vaccine are constantly being developed and tested. A highly promising one is a test of proteome. Levels of protein expression have been evaluated in precancerous lesions in the bladder of an *in vivo* rat

model. The predictive proteins are Rab-GDIβ, aldehyde dehydrogenase 2 and 14-3-3ζ/δ[58]. Another approach to prediction of BCG vaccine functionality and effectiveness is the computational mathematical model, which extracts information from empirically collected data on dosage and instillation schedule and predicts response of BCa patients to the treatment[59].

2.4. TB and LTBI diagnostic methods currently used in the clinic

Any mimicry between the tumor-specific antigens and the *M. bovis* antigens may further enhance the immune response and aid in the timely and more precise detection of BCa-responsiveness in patients. Therefore, the knowledge regarding diagnosis of TB and detection of LTBI carries a great potential for BCG instillation as treatment for BCa.

2.4.1. Tuberculin skin test

The most commonly used test in detecting TB and LTBI caused by *M. tuberculosis* is the tuberculin skin test (TST) alongside with an X ray examination. TST is performed by cutaneous injection of *M. tuberculosis* purified protein derivative (PPD) and the subsequent measurement of the local immune response[60]. Its great disadvantage is the low specificity in BCG vaccinated individuals. Moreover, the specificity of TST has been shown to be age specific. During childhood it decreases down to 62.7%[61] and this specificity perseveres into adulthood[62]. The guidelines of American Thoracic society, suggest to opt for alternative to TST in BCG vaccinated patients from the age of 5 years on[63]. In patients with active TB sensitivity of the TST was 25% and specificity 67%[63].

Therefore, the TST is not a sufficient method to detect the LTBI and identify the point of transition between LTBI and active TB. It must be complemented by other methods or replaced by a more efficient test. TST has also been performed in the course of treatment of BCa before the BCG vaccine was installed. 5-year survival rate was 66.6% of patients, who underwent the TST before BCG vaccination compared to 59.1% in the cohort, which did not undergo the TST[64]. Showing the enhancement property of TST for the efficiency of BCG instillation.

2.4.2. Interferon γ release assay (IGRA)

Interferon γ release assays (IGRA) is routinely used to confirm the TST positivity. IGRA has also been employed as an alternative or complement to the TST in cases where TST is not the best option due to factors listed above[65]. IGRA are based on enzyme-linked immunosorbent assay (ELISA). T cells are stimulated by *M. tuberculosis* peptides and the IFNγ release is measured. To account for the fact that the BCG vaccination interferes with the results of the TST, *M. tuberculosis* specific antigens have been identified, namely CFP-10 and ESAT-6 to increase both the specificity and the sensitivity of the tests. These antigens are not present in the BCG vaccine and therefore serve as unique indicators of the infection, which are not skewed by the BCG vaccination.

Currently the most commonly used IGRA are QuantiFERON-TB-Gold PLUS (QFT Plus), QuantiFERON-TB-Gold in tube and T-SPOT.TB. The sensitivity is 80.2% and 91% respectively[66]. In a low-risk study group, the sensitivity of QFT Plus was 87.93% and specificity was 97.17%[67].

However, in an attempt to increase the effectiveness of BCG vaccination, ESAT-6 has recently been added into the newly produced vaccine. This addition led to development of ESAT-6 free IGRA, which tested both new *M. tuberculosis* antigens, EspC, EspF and Rv2348c and IP-10 as a replacement readout for IFNγ. This new test shows highly promising results compared to QuantiFERON, which was used as a control (79% vs 84% sensitivity and 97% vs 99% specificity respectively)[68].

2.4.3. Monitoring of lymphocyte activation and cytokine release detection

Finally, TB can be highly accurately diagnosed by detection of cytokine release. A panel of cytokines was tested to determine which ones have the capacity to distinguish between LTBI and active TB. The panel included Il-1β, IL-2, IL-6, IL-10, IL-17, G-CSF, IFN-γ, IP-10, MIP-1α and TNF- α. IL-2, IL-10, IFN-γ, IP-10 and TNF- α levels were significantly higher in the LTBI patients[69].

IL-2 is a particularly useful marker, which has been tested in a method called LIOSpot, based on the ELISA method the same way as QuantiFERON method. In LIOSpot IL-2 levels are measured instead of IFN-γ release. ESAT-6 and CFP-10 were used as stimulants in the LIOSpot method as well, reaching sensitivity of 86% and 80% for the respective antigens and specificity of 36% and 54%. However, an additional marker, alanine dehydrogenase (Ala-DH) was included in the mix of stimulation antigens and the sensitivity was 96% and specificity 100%, which makes it a useful tool for active TB detection[70].

Another test, which has been proposed as a potential candidate to be combined with IGRA is TNF-α release assay (TARA). TARA in combination with IGRA led to increase in specificity to 93% for active TB and the sensitivity of 89%[71].

Finally, a test has been designed, which combines detection of IL-2, IFN-γ and TNF-α as LTBI specific markers. This triple marker test provides highly specific results, which enable more accurate diagnosis and detect LTBI with sensitivity >88%[72]. essences

2.5. Principles for designing a TAT panel

The goal of urological oncologists is to prescribe the right therapy, efficiently monitor progress of treatment and cure the patient. Flow cytometry offers a personalized approach, thanks to the single cell analysis and testing of large panels of markers, which may be adjusted based on patient's individual needs, medical history and immune profile. FCM provides an alternative to the currently used methods for a more accurate diagnosis and disease monitoring. It has been proved in literature that FCM is a robust method for detection of rare antigen-specific T cell populations[73]. In order to develop an efficient panel of markers to detect T cell specific activation, two major conditions must be met. The first one is the right selection of markers to be included in the panel and the second is the right stimulation of T cells to test the expression characteristic for BCa and LTBI with a high enough predictive value.

2.5.1. *In Vitro* T cell stimulation

The general frequency of antigen-specific reactive T cells has been detected ranging from 0.002% for epitope-specific reactive T cells to 1.73% of PPD reactive T cells in patients with active TB. The range is based on the type of antigen (tumor, BCG antigens, tuberculin, multimers bound to MHC), detection method (FCM, multimer binding assay) and origin of T cells (healthy donors, donors diagnosed with a tumor, donors with LTBI, donors with active treated vs non-treated tuberculosis)[74–76].

The PBMC isolated from whole blood or buffy coat must be set in culture (RPMI 1640 medium) and activated (by various stimuli). There are three major types of stimulants. T cells can be activated in a polyclonal, oligoclonal and monoclonal manner. Polyclonal stimulation leads to the largest number of activated T cells, oligoclonal comes second and finally the lowest number of T cells is activated by the monoclonal stimulation. This is the reason to move from polyclonal, to oligoclonal and finally to monoclonal stimulation in the development of TAT to test the detection power of the panel on increasingly challenging activators. To build and run the first tests on TAT panel I used the polyclonal activation.

PMA activates protein kinase (PKC) pathway and the ionomycin increases the intracellular levels of Ca^{2+}. PMA/ionomycin activation was selected to set a baseline of positive controls for the final TAT because it has been identified as the strongest stimulation to detect cytokine production and other activation markers. The expected response of T cells to polyclonal stimulation is up to 100%[77].

The oligoclonal stimulation is performed by so called superantigens[78]. The superantigens stimulate T cells by crosslinking Vβ part of the TCR and the MHCII molecule on APC[79]. Superantigens are used at a concentration ranging from 0.1 to 1000 ng/ml[80–82]. Oligoclonal stimulation leads to activation of up to 20% of $CD4^+$ and $CD8^+$ T cells combined[83].

Stimulation with the *Cytomegalovirus* (CMV) lysate represents a middle step in the process of detection of rare antigen-specific T cell populations, reaching 5 to 10% of all $CD8^+$ T cells[84]. Based on their origin 40%-90% of people are CMV positive, which ensures a sufficient proportion of CMV positive donors among healthy blood donors to serve as a

control[85]. Moreover, CMV lysate has been used as a powerful marker for prediction and monitoring of patient's response to selected immunotherapy[86].

The last type of T cell stimulation is antigen-specific or monoclonal. Monoclonal stimulation leads to the lowest numbers of reactive T cells in healthy individuals reaching only 0.01%[87]. The T cells are stimulated by specific antigens, at various concentrations based on the type of the antigen. Individual clones of reactive T cells are detected. In the TAT stimulation, the antigens will come from several sources, the BCG vaccine lysate, *M. tuberculosis* specific synthetic peptides and PPD, the BCa cell line lysate and the tumor lysates.

The BCG lysate represents antigens present in the BCG vaccine, which have the potential to trigger immune response. The tumor-specific antigens will follow in the form of BCa cell lines lysates and BCa patient sample lysates, to detect BCa-specific T cell activation in the personalized setting on patient's peripheral blood. Each stimulant will be used for *in vitro* test to detect the response in healthy BCG-vaccinated/non-vaccinated donors and compare it to the response mounted by latent and acute TB patients and BCa patients before and after BCG instillation. Healthy, adult donors serve as a control for the other cohorts.

2.5.2. TAT panel makers

As was described above, the T cell immune response is crucial for the success of prescribed immunotherapy. Based on the published research, I selected the following combination of markers to be included in the TAT panel.

Lineage markers

CD4 and CD8 are the most commonly used markers to detect T cell populations[88–93]. Other frequently used marker is CD3[88–93]. I decided to use all three markers, CD3, CD4 and CD8 because they provide a precise distinction of the T cell population.

Degranulation markers

As was stated above, the first manifestation of PBMC activation is degranulation and particularly degranulation of basophils[21,94]. Therefore, it is used as the primary initial control of successful stimulation as early as 1-hour after activation[95,96]. Numerous studies

on degranulation have been conducted and led to development of basophil activation test (BAT). The BAT is primarily used for detection of allergies[97] but has also been used to determine the oversensitivity of cancer patients to oxaliplatin chemotherapeutic[98] . Markers included in the BAT are CD63 (LAMP-3) and CD203c (ENPP3)[99] . CD 63 is present intracellularly on the membrane of granules in basophils, mast cells and platelets as well as on the membrane of other cells and is detectable on the surface after degranulation[100]. Degranulation is also an essential part of the initiation of cytolytic functions of T cells. Two markers, CD107a (LAMP-1) and CD107b (LAMP-2) have been shown to directly connect to the T cell cytolytic function mediated by perforin granzyme activation[101]. CD107a is a marker of both NK cells and T cell activation[102].

To include both the earliest markers and the T cell specific markers, CD63 and CD107a were included in the TAT panel. To avoid false positive signal in a T cell oriented assay, caused by platelets and basophils CD41 (ITGA2B) can be added to clearly distinguish platelets from a whole blood sample[103].

Activation markers

Alongside the initial degranulation, there are numerous surface activation markers, which are expressed on T cells after activation. A wide array of markers including CD25 (ILR2A), CD26 (DPP4), CD71 (TFRC), CD154 (CD40LG), CD69 and costimulatory molecules CD26, CD27, CD28, CD30 (TNFSF8) and CD134 (TNFRSF4). The markers can be divided into early and late activation markers, based on the time when they are expressed relative to the point of initial T cell stimulation.

The earliest one is CD69, a C-type lectin, which was shown to work as a powerful Due to its early expression and essential role in T cell activation it has been included in the TAT panel.

Two major late activation markers are CD137 (TNFRSF9) and CD154[104]. CD137 belongs to the TNF-receptor family and plays an important role in clonal expansion[105]and is expressed after T cell reacts in an antigen-specific manner[106]. CD137 has been identified as signature of activated T cells, my interest being particularly with the focus on tumor- and *M. tuberculosis*- specific T cells[35,107]. CD137 has been shown to identify tumor infiltrating lymphocytes with higher accuracy than previously thought PD-1[108], which may

be further increase the predictive value of the marker in future research. Although CD137 is expressed on both $CD4^+$ and $CD8^+$ T cells, in general there is a tendency to preferentially use is as a marker for $CD8^+$ T cells reactivity [109].

CD154 plays a role in T cell proliferation and cytokine production as a costimulatory agent by CD28 costimulation[110] and tyrosine phosphorylation[111]. CD154 is a marker of antigen-stimulation of $CD4^+$ T cells[112]. CD154 has been effectively used to define a population of T cells with an antiviral function[113].

Cytokines

Cytokines are small signalling proteins, which play an essential, irreplaceable role in immune response. Numerous studies have been conducted on identifying cytokines, which are specifically released after activation of T cells. Based on the previously reported literature search I decided to include IL-2, IFN-γ and TNF-α into the final TAT panel. These three cytokines have been previously used for detection of BCG-reactive responses and used for prediction of BCa patients' response to BCG therapy[114]

IL-2 is a major T cell cytokine. It leads to activation and expansion of T cells through TCR signalling. Activated $CD4^+$ and $CD8^+$ T cells produce IL-2. It has been shown that IL-2 can also play a role in self-tolerance. IL-2 influences $CD4^+$ $Foxp3^+$ subset, which has immunoregulatory function, making it an ambivalent cytokine in the sense that it induces T cell proliferation but resulting in both enhancement and suppression of immune response[115]. MAPK, JAK/STAT and PI3K/AKT pathways lead to synthesis of IL-2. When naïve $CD8^+$ T cells undergo activation and proliferate in the presence of IL-2, they are limited in development of effector function[116]. Overall the IL-2 is a marker of activation of T cells of various subsets, which makes it an excellent cytokine to be included in the TAT.

The second included cytokine is IFN-γ. IFN-γ is a proinflammatory cytokine, produced by NK and T cells in response to tumors and intracellular pathogens. It is associated with polarization towards Th1 response, which is essential in BCG vaccine therapy [117].

The last cytokine to be included is TNFα. TNFα is also proinflammatory but has ambivalent functions. TNFα works by activating the NFκB signalling pathway[118]. It belongs among the activation cytokines, which indicate antigen-specific T cell response[119].

At the same time it has been shown to inhibit $CD8^+$ T cell anti-tumor function[120]. TNFα is also important for the induction of MDSC by non-activated $CD4^+$ T cells, contributing to the induction of immune response[121]. This means that it also functions as a potent link between innate and adaptive immunity.

3. Goals of the experimental part of the diploma thesis

- Design a panel to detect T cell specific activation based on T cell specific markers, early and late activation markers and cytokines
- Optimize positive controls for the detection of non-specific polyclonal stimulation of T cells
- Use of uniCAR T cell system as a potential T cell specific positive control
- Detection of Ag-specific response to CMV stimulation

4. Materials and methodology

4.1. Materials

4.1.1. Cells

- Whole blood obtained from healthy donors
- Buffy coats from Institute of Hematology and Blood Transfusion (UHKT), donors #18002635, #18003342, #18003345, #18005433, #18005434, #18005439

4.1.2. Beads

- Rainbow Calibration Particles, 8-peak, Spherotech Inc. (USA), Cat. No. RCP-30-5A, Ref.No A79016, Lot.No.: AF02
- VersaComp Antibody Capture Bead Kit, Beckman Coulter (USA) Ref. No. B22804, Lot. No.: 4131002K
- CytoFLEX Daily QC Fluorospheres, Beckman Coulter (USA) Ref. No. B53230, Lot.No.: AJ06F, AJ02F

4.1.3. Antibodies

Table 1. Overview of used antibodies

Antigen	Clone	Fluorochrome	Manufacturer	Cat. No.	Concentration (μg/ml)	Final dilution
CD4	MEM-241	AF700	Exbio	A7-359-T100	unknown	1:320
CD8	MEM-31	Pacific Orange	Exbio	PO-207-T100	30	1:160
CD8	MEM-31	PE/Cy7	Exbio	T7-207-T100	30	1:320
CD8	MEM-31	PerCP/Cy5.5	Exbio	T9-207-T100	unknown	1:320
CD63	MEM-259	PerCP/Cy5.5	Exbio	T9-343-T100	unknown	1:160
CD107a	REA792	APC/Vio770	Miltenyi Biotech	130-111-623	205	1:320
CD69	FN50	FITC	BioLegend	310904	unknown	1:160
CD137	4B4-1	BV650	BD Biosciences	309828	100	1:40
CD154	24-31	PE	Exbio	1P-781-T100	100	1:20
IFNγ	4S.B3	APC	Exbio	1A-706-T100	unknown	1:10
TNFα	MAb11	BV605	BioLegend	502936	unknown	1:20
IL-2	MQ1-17H12	PE/Cy7	BioLegend	500326	100	
CD41	MEM-06	PB	Exbio	PB-309_T100	1243	1:160
E5B9 antibody	Laboratory of professor Bachmann				unknown	1:20
GAM-PE						

4.1.4. Buffers and chemicals

Table 2. List of used reagents

Reagent	Distributor	Cat. No.	Lot. No.
HBSS	IMG ASCR		
PBS			
Gelatine	Sigma-Aldrich	G7765-250ML	SLBH6724V
Sodium azide	Sigma-Aldrich	S8032-25G	BCBQ2297V
Ficoll-Paque™PLUS	GE Healthcare Biosciences AB	17-1440-02	10225938
DMSO	Sigma-Aldrich	D2650-100mL	RNBF8134
Ionomycin	Sigma-Aldrich	IO634	080430
PMA	Sigma-Aldrich		
PHA			
CMV lysate	2nd Medical Faculty CUNI, doc. Kalina		
Triton X-100	Sigma-Aldrich	T8532-100mL	033KD0605
Paraformaldehyde	Sigma-Aldrich	P6148-500G	010M1507
Hoechst 33342			
Hoechst 33258			
Fetal Calf Serum (FCS)	Biosera		
RPMI	Sigma-Aldrich	R8758-500ML	RNBF9794
BD FACS Permeabilizing Solution2	BD Biosciences	340973	6357992
BD FACS Lysing Solution	BD Biosciences	349202	8059717
Brefeldin A	eBioscience	00-4506-51	E00021-1633

- I used 1x HBSS with bicarbonate (23.3.mL/500mL 1xHBSS) for work with cells in RT in the laboratory.
- I stained cells with antibodies in 1xHBSS with bicarbonate, 0.1% gelatin and <0.01% sodium azide

4.1.5. Laboratory equipment

- Microscope Olympus CHA, Olympus (Japan)
- Carl Zeiss Primo Vert™ inverted microscope, Carl Zeiss AG (Germany)
- Classic vortex mixer, Velp Scientifica (Italy)
- Centrifuge Alegra X-15R, Beckman Coulter, Inc. (USA)
- Shel Lab CO_2 incubator, Sheldon Manufacturing, Inc. (USA)
- 13-parameter CytoFlex S, Beckman Coulter, Inc. (USA)
- MacsQuant Analyzer, Miltenyi Biotech (Germany)

4.1.6. Software

- CytExpert v2.1., Beckman Coulter, Inc. (USA)
- Flow Jo, v10.5.3, FLOWJO, LLC (USA)
- MacsQunatify SW, Miltenyi Biotech (Germany)

4.1.7. Laboratory consumables

- Pipetman®Classic, P2, P10, P20, P100, P200, P1000, Gilson (USA) certified at Sipoch
- Gilson tips, Diamond for pipetman, Gilson (USA), Ref.No. F171200, F171300
- Lithium Heparin Vacuettes for blood donations, Greiner bio-one (Austria), ref.no. 456083, Lot. No.: A17013SM
- Culture flasks 50mL, SigmaAldrich (Germany), Ref.No. CLS432150
- Culture flasks 75mL, SigmaAldrich (Germany), Ref.No. CLS3290
- Serological disposable pipets, 10mL, Fisherbrand (USA), Cat. No. 13-676-10J
- Serological disposable pipets, 5mL, Fisherbrand (USA), Cat. No. 13-676-10H
- 6-well plates, Corning (USA), Cat.No. 3506
- 96-well polypropylene plates, Fisherbrand (USA), Cat. No. 12565502, Lot. No.: 155238
- Plastic tubes 15mL, Fisherbrand (USA), Cat. No. 05-539-5
- Plastic tubes 50mL, Fisherbrand (USA), Cat.No. 05-539-7
- Cryogenic vials, Biologix (USA), Cat.No. 81-7204, Lot.No. 120702

- Vials 1,5mL, Eppendorf (Germany), Cat.No. 0030123328
- Vials 2mL, Eppendorf (Germany), Cat. No. 0030123344

4.2. Methodology

4.2.1. Isolation of peripheral blood mononuclear cells (PBMC) using Ficoll Paque gradient

The PBMC were isolated from whole blood and from buffy coat obtained from healthy donors. In order to isolate PBMC I used FicollPaque and followed the protocol provided by GE Healthcare. First the 45 mL buffy coat is diluted with 1x HBSS to achieve the final volume of 80 mL. 10 ml Ficoll Paque is put into a fresh 50ml tube and then carefully layered over with 40 mL of prediluted buffy coat. The final ratio of Ficoll Paque to diluted buffy coat is 1 to 4. This way, each buffy coat is processed in two 50ml tubes. The tubes are carefully placed in a centrifuge and spun down at 400 g for 30 minutes at 20 °C with minimal acceleration and deceleration and no brake. The layer of white blood cells forms a clearly visible white ring above the layer of Ficoll Paque and it must be carefully transferred to a fresh 50ml tube and washed once in 1x HBSS with bicarbonate.

In order to detect lymphocyte-specific degranulation the platelets must be very carefully identified and eliminated because they express both degranulation markers CD63 and CD107a themselves[122]. Since there are 150-400∗10^6/ml they can lead to false positivity in the cytometric measurement[123]. Additionally, platelets aggregate and attach to granulocytes, monocytes and lymphocytes after their degranulation, which further skews the results. Therefore, I tested staining with platelet-specific CD41 marker to exclude the platelet population[124] from whole blood samples. The resulting gating strategy is shown in *Figure 6* below. In blood processed on Ficoll Paque, the samples were centrifuged at 80xg for 20 minutes, which proved efficient enough. Cells are spun down to the pellet and the thrombocytes are discarded with the supernatant.

4.2.2. Stimulation of PBMC

The most potent non-specific polyclonal stimulus is phorbol 12- myristate 13- acetate (PMA) in combination with ionophore ionomycin. Based on literature research I opted for 20 ng/ml of PMA and 500 ng/ml of ionomycin. The stimulation was performed in the volume of 2ml, at $2*10^6$ cells/ml in 12-well plates for 6, 24, 120 hours at 37 °C, 5% CO_2[74–76].

4.2.3. Flow cytometry

Flow cytometry (FCM) is a method enabling the detection, analysis and description of a sample on a single cell level. Beckman Coulter CytoFlex S at the Faculty of Science flow cytometry facility has been used with the configuration shown in *Table 2*.

BC CytoFlex S uses Avalanche photodiode (APD) detectors as opposed to photomultiplier (PMT). The APD system uses gain, as a reverse function of voltage during sample acquisition. The gains were adjusted in order to ensure accuracy of measurements. To set the right gains, we have used a manual baseline determination for each channel where minimal CV has been achieved with increasing SD for BC calibration beads. Additionally, we have used Spherotech Rainbow beads and compared the position of 8 visible peaks on the scale.

A long-term reproducibility of measurement is ensured by performing quality control measument of CytoFlex daily QC fluorospheres before every measurement. The CytExpert software newly offers a setup standardization, which automatically updates acquisition settings after running the QC standardization procedure, however I have not used this feature for my experiments. The optimized settings are presented in *Table 4*.

4.2.4. Titration of monoclonal antibodies (mAb)

Antibodies from the designed panel must be titrated on PBMC isolated from buffy coats or whole blood. The PBMC were stained for extracellular (CD4, CD8, CD63, CD107a, CD69, CD137, CD154) and intracellular (IL-2, IFNγ, TNFα) markers. CD4 and CD8 were titrated on non-activated PBMC. CD63, CD107a, CD69, IL-2, IFNγ and TNFα were titrated on cells activated for 6 hours, CD137 and CD154 were titrated on cells activated

for 24 hours. All antibodies were diluted and PBMC were washed and measured in a staining buffer 1x HBSS with 0.1% of gelatine and <0.01% of sodium azide.

100 µl of PBMC suspension (from $6*10^6$ cells/ml), were transferred from 5ml tubes and washed in a 96-well polypropylene plate. The staining with individual antibodies is performed on a pellet of PBMC. The serial dilution of antibodies is prepared in 10 µl of the staining buffer starting from 2x the concentration recommended by the manufacturer and then decreasing the concentration two-fold in each following well until the final dilution of 1 to 2560 in the final volume of 20 µl (pellet from left after centrifugation of 100 µl PBMC suspension from $6*10^6$ cells/ml and 10 µl staining solution with correct amount of added antibodies) was reached. After the serial dilution has been prepared for extracellular markers, the PBMC were incubated with antibodies for 30 minutes, in the dark at RT. After incubation, cells are washed by 350 µl of staining buffer, centrifuged at 300g for 5 min and resuspended in 100 µl of staining buffer for measurement.

For the detection of intracellular markers, Brefeldin A (BFA) is added to the PBMC 2 hours after the initial activation. Brefeldin A blocks the Golgi complex from pumping the produced cytokines to extracellular space. The PBMC were centrifuged at 500g for 8 minutes at RT. Next, PBMC were resuspended in 100 µL BD FACS Lysing solution and incubated for 10 minutes in dark at RT, then they were centrifuged at 500g for 8 minutes at RT again and resuspended in 200 µL of BD FACS Permeabilizing Solution 2 and incubated for 7 minutes in dark at RT. The permeabilized cells were centrifuged at 1500g for 8 minutes at RT and stained with intracellular antibodies. Intracellular antibodies were incubated for 30 minutes at RT, then the cells were washed and centrifuged as was described in the previous step. The final stained sample was resuspended in 100 µL of staining buffer and measured.

To analyze the acquired data and select correct dilution factor, the important parameter during measurement is the median fluorescent intensity (MFI) of both negative and positive populations calculated by the software. Correct gating is key in order to determine the best dilution to be used in future experiments. The measured MFI values are used to create the titration graph and calculate the stain index. Stain index determines the optimal dilution by identifying the point of best separation between positive and negative population of cells. See *Figure 7* and *Figure 8* for exemplary graphs.

$$\mathrm{SI} = \frac{MFI_{pos} - MFI_{neg}}{2SD_{neg}}$$

Equation 1. Calculation of stain index. *The Median fluorescent intensity of negative population is subtracted from the median fluorescent intensity of the positive population and the resulting number is divided by standard deviation of the negative population times two.*

Once the antibodies are titrated the optimal dilution is used for staining the PBMC in a total volume of 20 µl (pellet from left after centrifugation of 100 µl PBMC suspension from $6*10^6$ cells/ml and 10 µl staining solution with the right amount of added antibodies).

4.2.5. Compensation

Compensation is a mathematical operation that serves the purpose of right visualization and analysis of acquired data. The aim of compensation is to correct the overlap of individual spectra when using multiparametric panels for FCM[125]. The goal is to achieve the orthogonal distribution of populations to clearly separate them from each other and be able to identify all the expressed markers from the panel of antibodies specifically on each population, and each subset. In order to achieve the maximum attainable positivity, I used VersaComp Antibody Capture Kit. Equal proportions of positive and negative beads are mixed (3 drops each) and 10 µl of the solution with beads are stained with antibody in the final volume of 20 µl. The beads are incubated in the dark, at RT for 20 minutes, washed with staining buffer and measured. The cells of interest are stained with the entire panel of antibodies, incubated at RT in the dark for 30 min. After incubation, cells are washed in 350 µl staining solution, centrifuged at 300g for 5 minutes and measured on CytoFlex S using CytExpert software applying the calculated compensation to analyze the data.

Since the manual setup is prone to introducing errors into the calculation, the trend is to establish an automated workflow to ensure accuracy and reproducibility of experiments[126].

4.2.6. Cell line cultivation

For the purposes of working with uniCAR system, I was trained in cell line cultivation. In order to be able to establish a positive control using the uniCAR T cells, two cell lines, were selected, PC3 and LNCap both from the laboratory of professor Michael Bachmann

at Carl Gustav Carus Institute in Dresden, Germany. Both PC3 and LNCap cell lines are prostatic adenocarcinoma cell lines and were selected for the expression of PSCA[128,129]. PC3 and LNCap cell lines have been set in culture and cultivated in an incubator at 37 °C and 5% CO_2. The cell lines were cultivated in RPMI 1640 medium with 10% FCS and 100 mg/mL of streptomycin.

4.2.7. SDS-PAGE Electrophoresis

The SDS-PAGE electrophoresis is a method used to separate proteins. The separation occurs on a polyacrylamide gel in the presence of sodium dodecyl sulfate (SDS). The gel is prepared following the protocol in a fume hood. The final gel consists of stacking and separating part, which differ in the amount of individual chemicals shown in *Table 3*.

Table 3. Preparation of SDS-PAGE gel

	Stacking gel (μl)	Separating gel (μl)
H_2O	2975	4600
5M Tris-HCl	1250	2600
30% acrylamide	670	2600
10% SDS	50	100
10% ammonium persulfate	50	100
TEMED	5	10

The gel was left to polymerize for 30 to 40 min and then was stored in water or wet towel in a fridge overnight for later use. To determine the amount of protein, known amount of Bovine serum albumin (BSA) standards were used as a reference sample in a serial dilution prepared from stock concentration of 10 μg/μl into final volume of 10 μl. The serial dilution was: 0.25 μg, 0.50 μg, 1 μg, 3 μg, 5 μg and 7 μg. The protein had to be denatured at 95 °C for 10 min before loading onto the gel. After the protein was loaded, the gel ran at 80 V for 10 to 15 min, for the samples to enter the gel. After that the voltage was increased to 100-120 V and the gel ran for 60 to 90 min (until the bands were clearly separated). To visualize the sample, the gel had to be stained with Coomassie Brilliant

Blue (Coomassie Brilliant Blue 0.25 g, 10% acetic acid, 20% methanol) for 60 minutes at RT and de-stained using de-staining solution (20% methanol and 10% acetic acid) three times for 30 minutes and left overnight at RT.

4.2.8. Western blot

The Western blot is an analytical method used to detect specific proteins. The protein, which underwent SDS-PAGE electrophoresis is transferred onto a membrane, using 15 V for 60 min. The membrane is blocked and stained with primary antibody. Primary mouse antibody targeted against E5B9 and PSCA were used at a concentration of 5 μg/mL. After the first staining blocking solution of Bovine Serum Albumin (BSA) is used on a shaker for 60 min at room temperature (RT). Then the membrane continues to secondary GAM antibody staining at a concentration 0,5 μg/mL. Finally, the bands were detected using Image Lab software.

4.2.9. Binding assay

The binding assay is a technique which serves to prove the presence of TM through detection of E5B9 peptide by a specific mAb for the binding assay, 96 well plates are used. 200 000 target cells/well (cancer cells) in 50μl and serial dilution (two-fold) of TM in PBS starting at 125 μg/mL were used. The cells were incubated with TM at 4 °C for 60 min. After the incubation wells were washed twice with PBS and centrifuged at 360x g for 3 min and incubate the sample with antibodies against E5B9 epitope followed by a secondary GAM IgG antibody conjugated with PE fluorochrome. After antibody staining and 2 rounds of washing, the cells are measured on a cytometer to detect positivity for PE-conjugated antibody. This method serves to prove the presence of TM target molecule on the surface of a tested cell line and leads to calculation of equilibrium dissociation constant, K_D. K_D is essential for determining the affinity of TM to the target cells and the effectivity of the CAR T cells.

5. Results

5.1. Design of TAT panel

I designed the TAT panel for future use in diagnosis and monitoring of BCG vaccine therapy. I designed the panel using FluoroFinder software (https://fluorofinder.com/). The original complete panel included all selected parameters measurable at once (*Table 4*).

Table 4. Design of complete TAT panel for BC CytoFLEX. *The table demonstrates set-up of BC CytoFlex cytometer for the detection of surface markers. Each marker is listed under the respective channel based on the fluorochrome to which it is conjugated, row "Label". I included the gain setup values in parentheses next to the label of each respective channel. Numbers listed in the row titled "Filter" represent the parameters of bandpass filters for each respective channel. Blue background indicates T cell core markers, orange are degranulation markers, red surface activation markers and yellow cytokines.*

BC CytoFLEX setup (FacSci CUNI) **COMPLETE PANEL**							
VIOLET 405		V1 (300)	V2 (500)	V3 (1000)	V4 (2800)	V5	V6
	Filter	450/45	525/40	610/20	660/20		
	Label	Hoechst	CD8_PO	**TNFα_BV605**	**CD137_BV650**	empty	empty
BLUE 488			B1 (150)	B2	B3	B4 (1200)	
	Filter		525/40			690/50	
	Label		**CD69_FITC**	empty	empty	CD63_PerCP/Cy5.5	
GREEN 561			G1 (800)	G2 (1300)	G3 (1300)	G4	G5 (3000)
	Filter		585/42	610/20	690/50		780/60
	Label		**CD154_PE**	CD3_PE/DL594		empty	**IL-2_PE/Cy7**
RED 637					R1 (3000)	R2 (3000)	R3 (3000)
	Filter				660/20	712/25	780/60
	Label				**IFNγ_APC**	CD4_AF700	CD107a_APC/Vio770

Because I made a mistake with CD8_PO, which resulted in running out of the antibody prematurely, I decided to split the panel into two mutually compatible panels. The first one covers surface activation markers and is presented in *Table 5*. The second resulting panel is focused on the detection of T-cell specific cytokines. Its design is depicted in *Table 6*. First, cells were stained with antibodies for T cell core markers on the surface and then cells were permeabilized and stained for cytokines.

Table 5. Surface markers panel. *The BC CytoFLEX gains set-up remained the same as the one demonstrated in Table 7. Only surface activation markers were included in the panel.*

BC CytoFLEX setup (FacSci CUNI) SURFACE MARKERS PANEL							
VIOLET 405		V1	V2	V3	V4	V5	V6
	Filter	450/45	525/40	610/20	660/20		
	Label				**CD137_BV650**	empty	empty
BLUE 488			B1	B2	B3	B4	
	Filter		525/40			690/50	
	Label		**CD69_FITC**	empty	empty	**CD63_PerCP/Cy5.5**	
GREEN 561			G1	G2	G3	G4	G5
	Filter		585/42	610/20	690/50		780/60
	Label		**CD154_PE**			empty	**CD8_PE.Cy7**
RED 637					R1	R2	R3
	Filter				660/20	712/25	780/60
	Label					**CD4_AF700**	**CD107aAPCVio770**

Table 6. Panel for cytokine detection. *The set-up of BC CytoFLEX gains remained the same as the one demonstrated in Table 7. T cell core markers were complemented with cytokine activation.*

BC CytoFLEX setup (FacSci CUNI) CYTOKINE DETECTION PANEL							
VIOLET 405		V1	V2	V3	V4	V5	V6
	Filter	450/45	525/40	610/20	660/20		
	Label			**TNFα_BV605**		empty	empty
BLUE 488			B1	B2	B3	B4	
	Filter		525/40			690/50	
	Label			empty	empty	**CD8_PerCP/Cy5.5**	
GREEN 561			G1	G2	G3	G4	G5
	Filter		585/42	610/20	690/50		780/60
	Label		**CD3_PE**			empty	**IL-2_PE/Cy7**
RED 637					R1	R2	R3
	Filter				660/20	712/25	780/60
	Label				**IFNγ_APC**	**CD4_AF700**	

To confirm that the gains were set correctly, I measured Rainbow 8-peak beads on the above listed gains. As shown in *Figure 5*, all the peaks fit on the scale when measured on the respective gains. All eight peaks must fit onto the scale while maintaining a good distinction between individual peaks. High values in all red channels, V4 and G5 result in the need for high compensation between the respective channels.

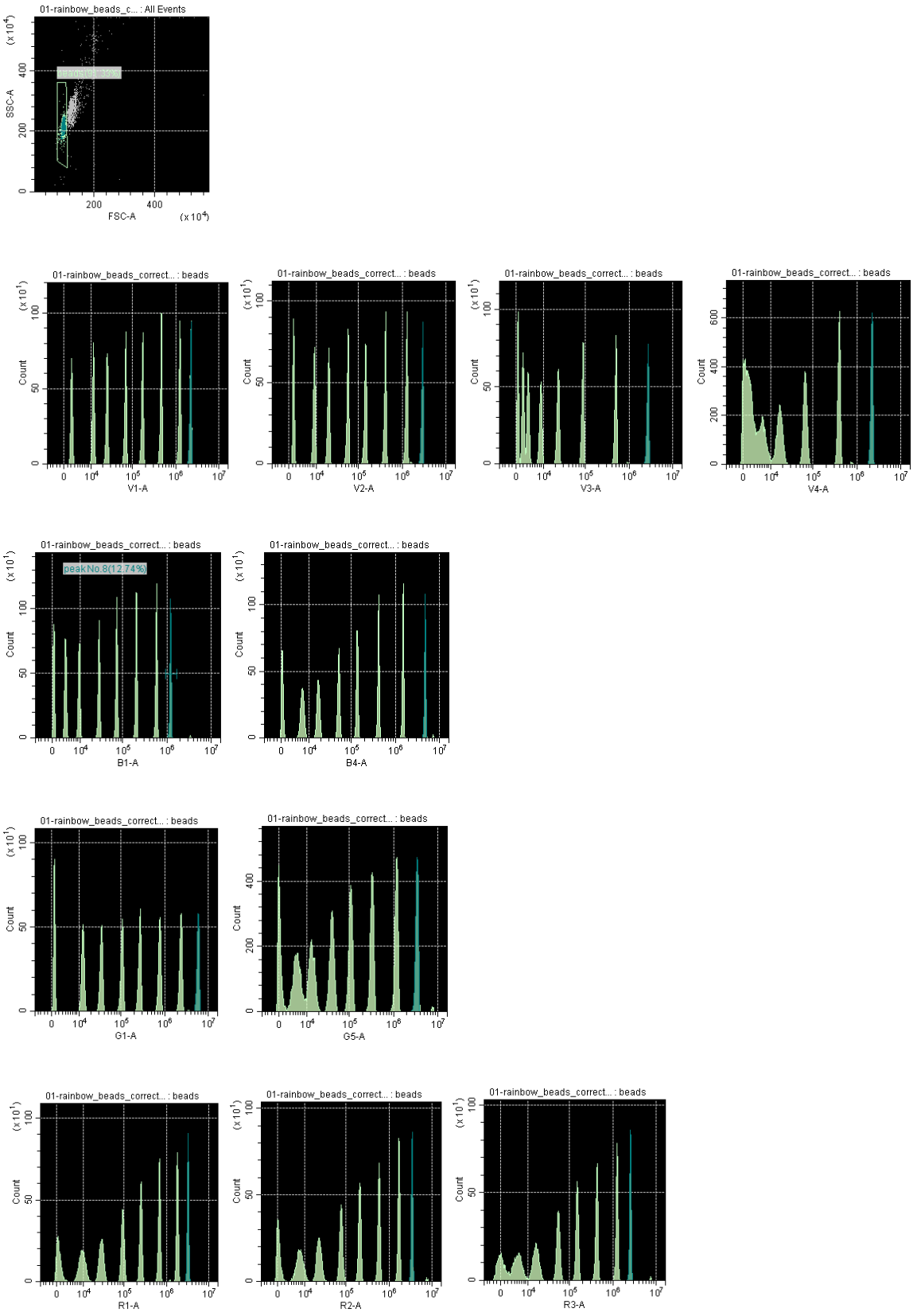

Figure 5 Control of correct gain setup. *Rainbow 8-peak beads were measured in all channels to confirm that the correct gains were set. The last peak is set in dark green.*

Gating strategy is essential for analyzing the data acquired on the target cell population. For the titrations I used gating strategy depicted in *Figure 6*.

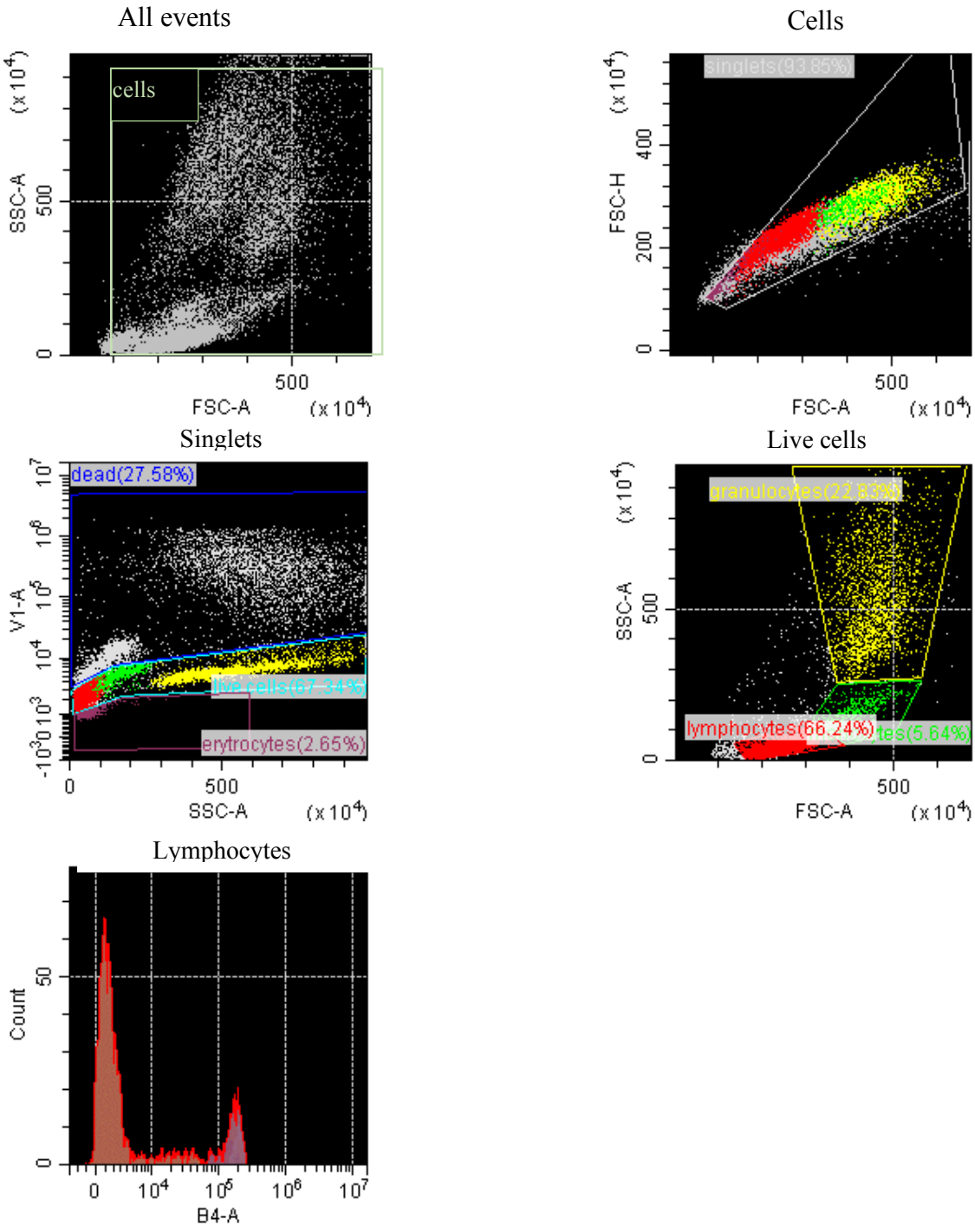

Figure 6. Gating strategy of non-activated lysed blood measured on BC CytoFLEX. *From all collected events depicted in the first dot plot, I gated on cells. Then I selected singlets on FSC-A vs FSC-H, in the form of typical conical singlet gate. Singlets were then visualized on a dot plot of SSC-A vs V1 (viability dye channel), where I gated on cells, which are negative for Hoechst 33342, shown in*

the light blue live cells gate. From the live cells I gated on individual populations of PBMC, based on the typical blood profile. Individual cell types were designated their own colors: Neutrophils (yellow), monocytes (green) and lymphocytes (red). The CD8 antibody was titrated on cells from lymphocyte gate, shown in the histogram.

For the purposes of calculating the compensation matrix and staining the cells correctly, the used antibodies must be titrated and used in constant final concentration. Each panel was compensated separately. The cells were stained in steps described in the methodology part of the thesis. The resulting SI calculated using the *Formula 1* and MFI of positive populations were put in separate graphs as shown in *Figure 7* and *Figure 8* respectively. The optimal dilution was identified and used in all following experiments.

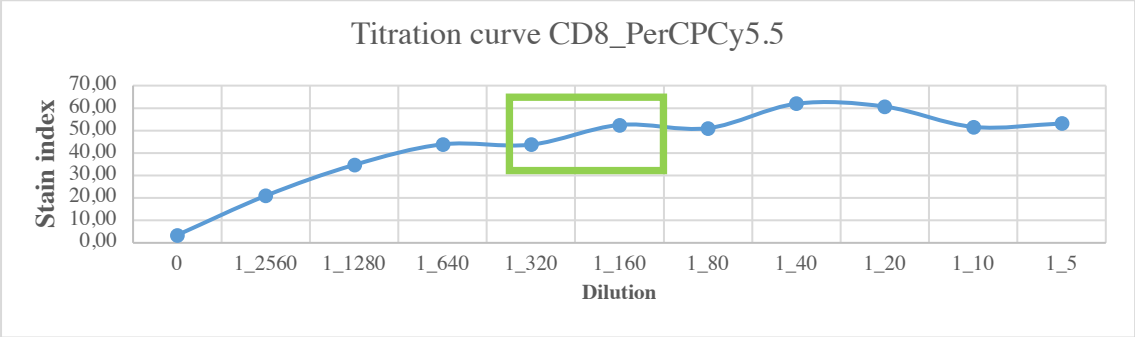

***Figure 7. Example of titration analysis of CD8 monoclonal antibody**. Each dot represents one dilution in the serial dilution of the titration. Figure represents the titration curve based on Stain index values.*

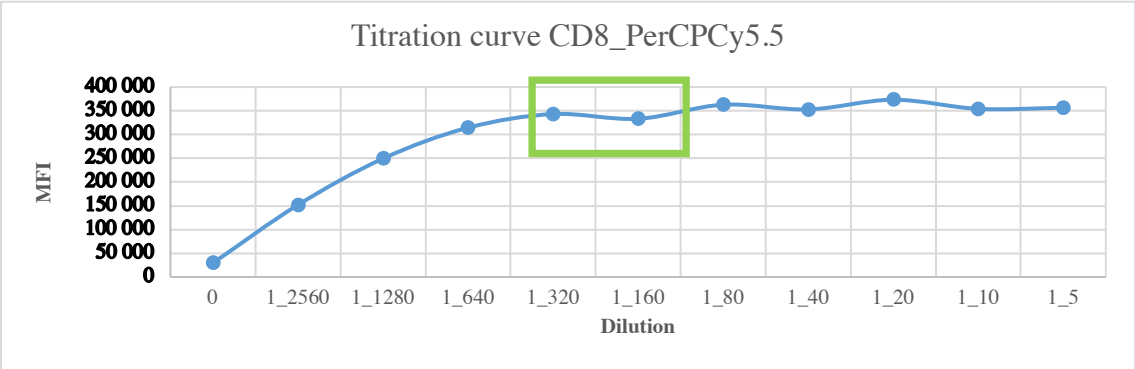

***Figure 8. Example of titration analysis of CD8 monoclonal antibody**. Each dot represents one dilution in the serial dilution of the titration. Figure 8 is for comparison, based on MFI values.*

When I repeatedly experienced difficulties with signal detection on positive controls for CD154_PE and TNFα_BV605, I tested whether the antibody is properly conjugated with

the right fluorochrome by staining positive and negative beads using a dilution of 1 to 10, shown in *Figure 9*. When the antibody is correctly conjugated with the fluorochrome, two sharp peaks (one for the positive and one for the negative population) are detectable in the respective channels, (CD154_PE in G1 and TNFα_BV605 in V3). The conclusion is that both antibodies are correctly conjugated and detectable using the channels, as expected on BC CytoFLEX.

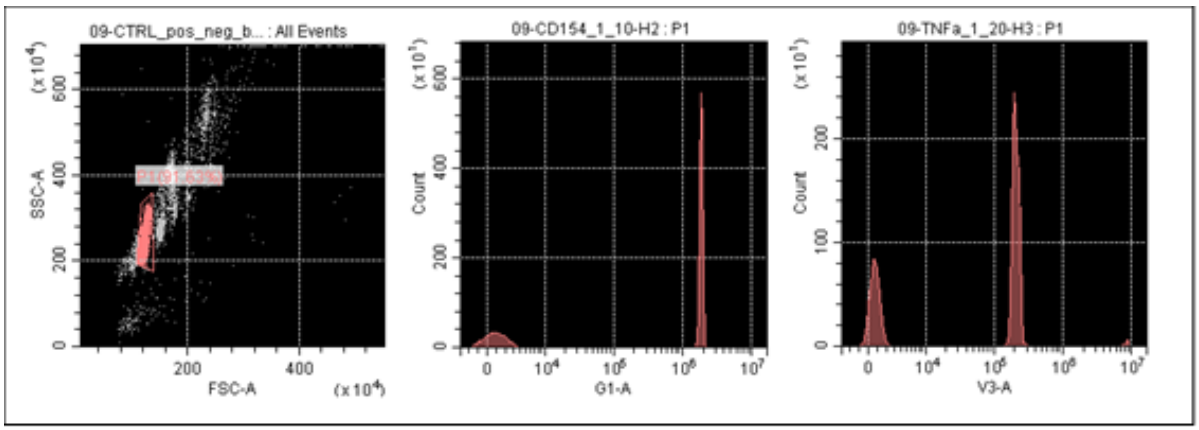

Figure 9. Control of conjugation of antibodies CD154 *(G1)* ***and TNFα*** *(V3).* ***.*** *The first dot plot shows the gating strategy for selection of beads. CD154 is detected in G1 channel and TNFα is detected in V3 channel on positive and negative beads forming the separate sharp peaks.*

Compensation matrix was calculated based on positivity detected using single stain controls on beads. The accuracy and applicability of the compensation matrix was analyzed based on two outputs. The first one is depicted in *Figure 10* and *Figure 11* for surface markers panel and cytokine detection panel respectively is the so called NxN plot. The goal is to achieve orthogonal distribution of populations. In surface markers panel (*Figure 10)*, there is a non-orthogonal distribution between R2 (CD4) and B4 (CD63) and between G5 (CD8) and R3 (CD107a). The NxN plot for cytokine detection panel (*Figure 11)*was based on correct matrix calculation correctly, achieving orthogonal distribution.

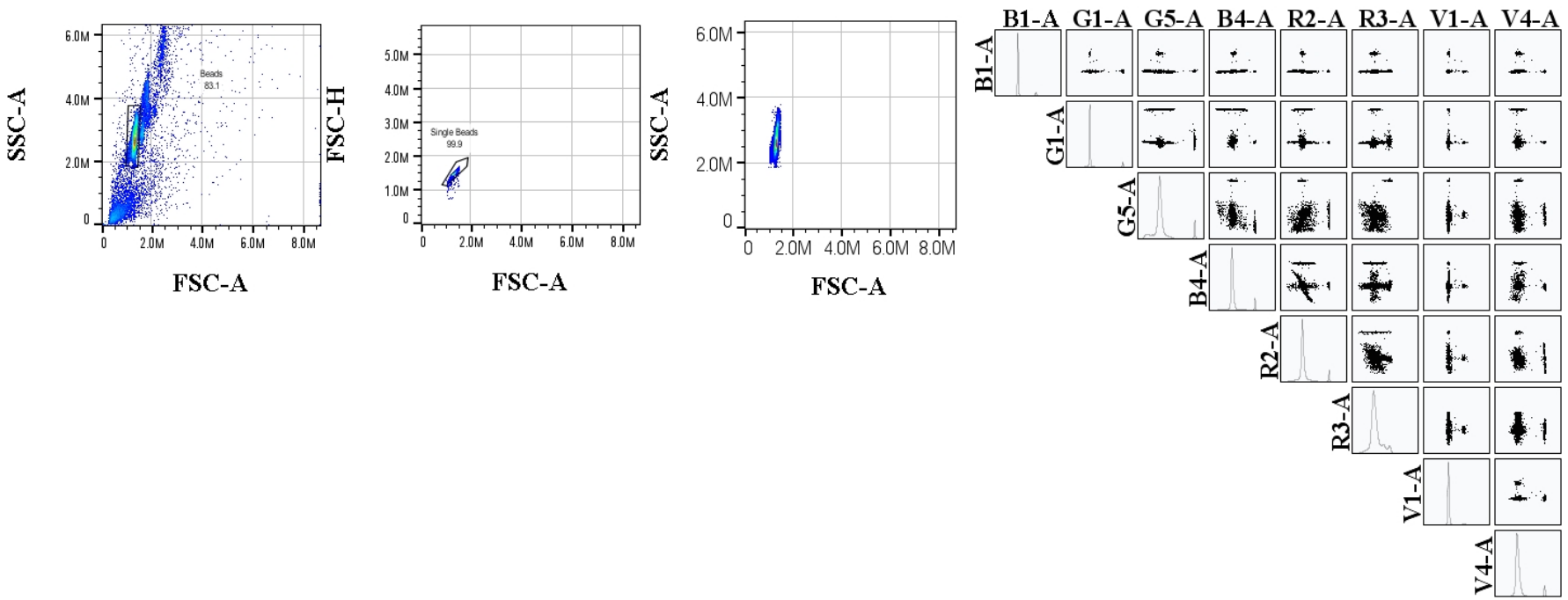

Figure 10. Compensation matrix for surface markers panel performed on conjugated beads*. The NxN plot illustrates the compensation matrix acquired in FlowJo software, which was applied to conjugated file of beads and then used for cell samples as well. The NxN plot shows the orthogonal distribution achieved using the compensation matrix.*

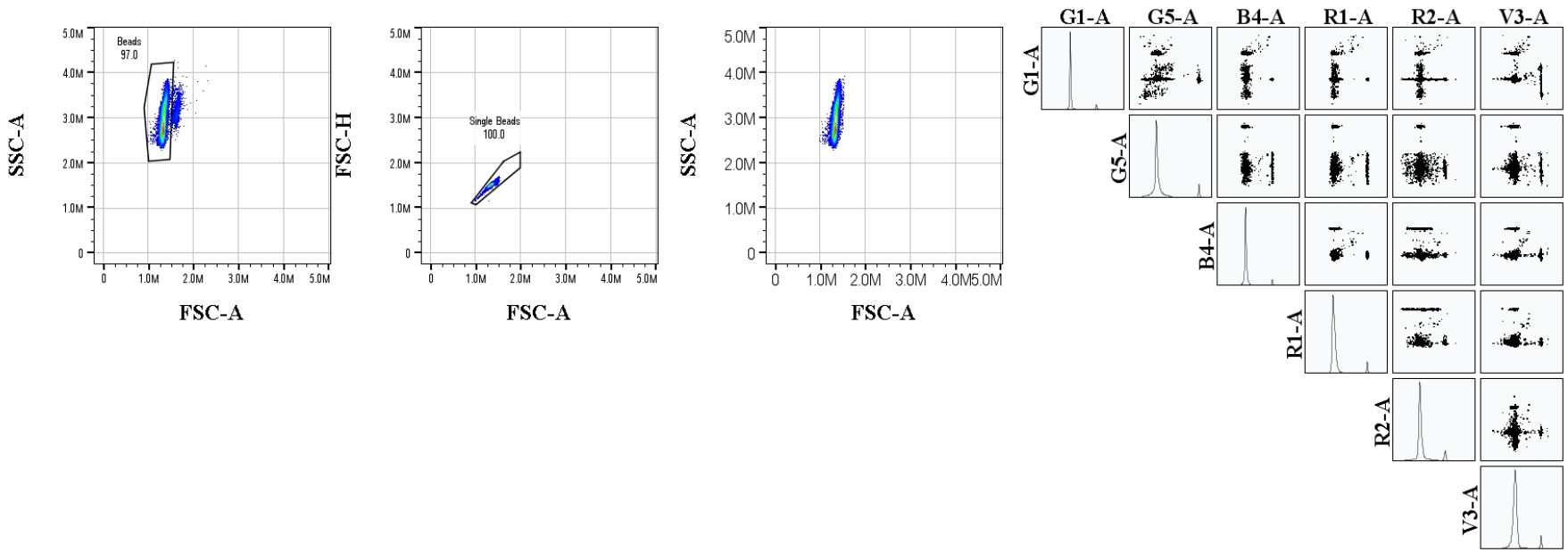

Figure 11. Compensation matrix for cytokine detection panel performed on conjugated beads*. The NxN plot illustrates the compensation matrix acquired in FlowJo software, which was applied to conjugated file of beads and then used for cell samples as well. The NxN plot shows the orthogonal distribution achieved using the compensation matrix. The individual populations of beads assume an orthogonal position to each other.*

A second type of visualization for correct evaluation of compensation matrix is based on analysis of the spillover among channels demonstrated in *Figure 12* and *Figure 13*. The panels were evaluated based on spread of the signal from each fluorochrome into the surrounding channels.

The spillover for surface markers panel, as shown in *Figure 12* is acceptable except for signal in G5 (CD8) and R3 (CD107a). Signal from G5 is not fully compensated and is detectable in R3 and the signal specific for R3 is undercompensated, which corresponds with the conclusion drawn from NxN plot of surface markers, *Figure 10*.

As shown in *Figure 13* there is no significant spillover among individual channels. However, there is a high background signal in particular in V3 (TNFα), G1 (CD3) and R1 (IFNγ). G5 (IL-2) channel has a high background signal originating from B4 (CD8), R1 (IFNγ) and V3 (TNFα).

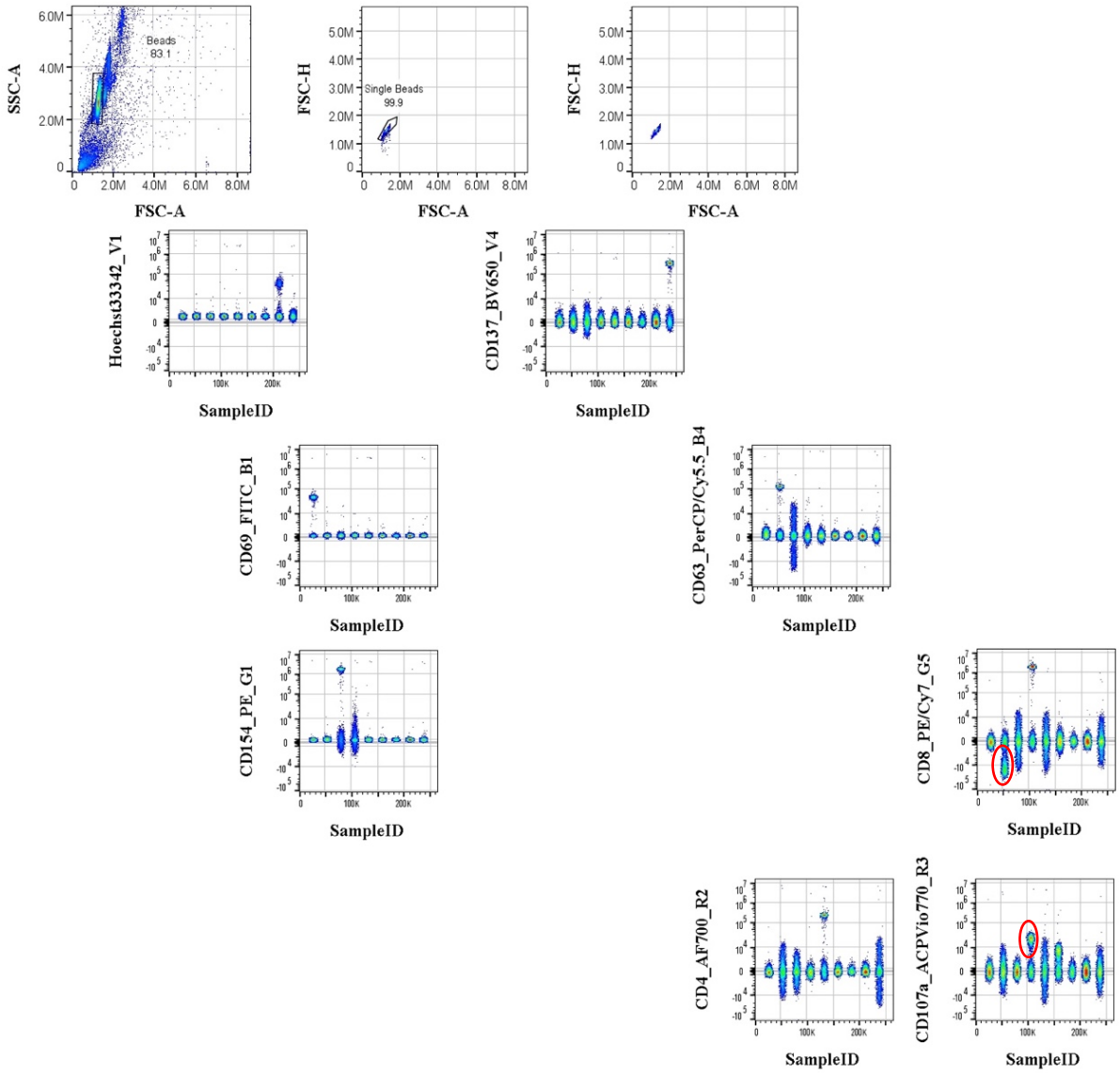

Figure 12. Depiction of spillover among individual channels for surface markers panel. *The layout mirrors the setup of lasers and individual channels in CytoFLEX cytometer as depicted in Table 7. Each pseudocolor plot represents a population of beads stained with respective antibodies as described in the annotation of each y-axis. Individual channels, on the x-axis B1, B4, G1, G5, R2, R3, unstained, V1, V4 labeled SampleID. The beads highlighted in red frame are overcompensated in G5 and undercompensated in R3.*

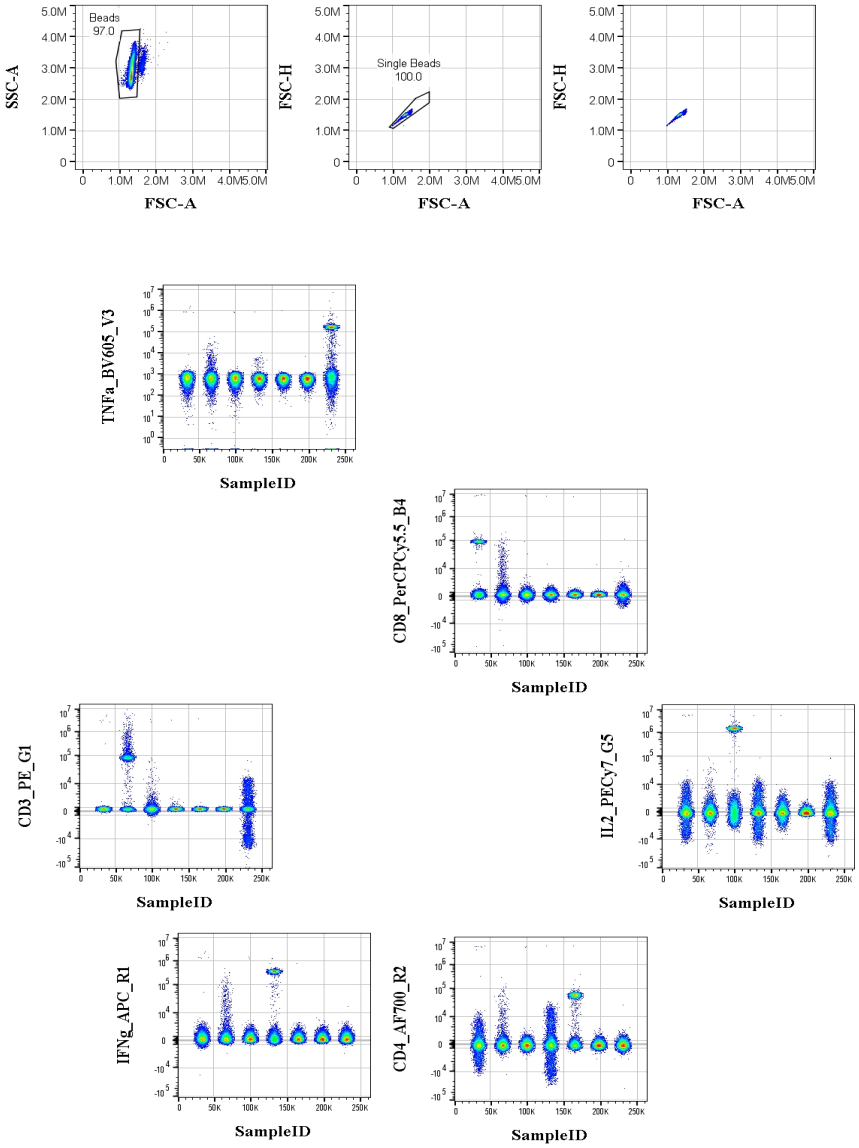

Figure 13. Depiction of spillover in between individual channels for cytokine detection panel. *Layout reflects the CytoFLEX cytometer setup as shown in Table 7. Individual channels on the x-axis are B4, G1, G5, R1, R2, unstained and V3 labeled SampleID.*

5.2. Detection of surface markers

I used the calculated compensation matrices for analysis of acquired data.

5.2.1. CD4 and CD8 expression in time

First, I focused on the detection of surface core T cell markers, CD3, CD4 and CD8. I measured the expression of T cell core markers in relation to activation at 4 time points (0, 1 hour, 6 hours and 24 hours post-stimulation) to evaluate their expression during the polyclonal stimulation with PMA/ionomycin. Non-stimulated samples were gated following the strategy presented in *Figure 14*.

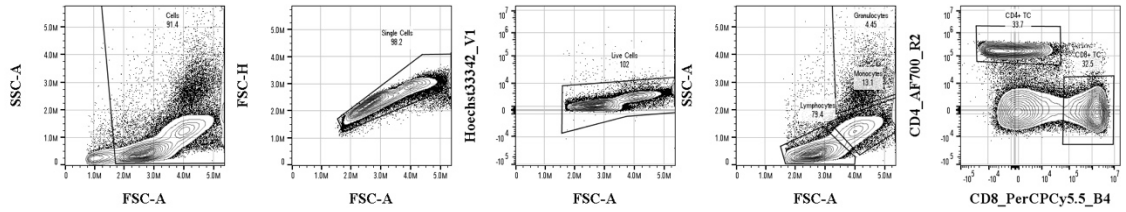

Figure 14. Gating strategy in FlowJo software for the analysis of both panels. *The first gate was set to include all the cells, and it was gated on FSC-A vs SSC-A. In the second step the singlets were gated in a typical conically shaped singlet cell gate on FSC-A vs FSC-H. The next step was to gate live cells from singlets based on their negativity for Hoechst, detectable in V1 channel. On the cleared data from live cells gated on FSC-A vs SSC-A, typical blood profile was established, and lymphocytes were divided based into CD4 and CD8 positive populations.*

When I stained lymphocytes with T cell core markers, CD4 was internalized after 6 hours of polyclonal stimulation with PMA/ionomycin. Once the CD4 marker internalized it was no longer possible to gate $CD4^+$T cells accurately, *Figure 15*. Therefore, when I expected $CD4^+$T cells to express surface activation markers I decided to gate the population as $CD8^-$, which included the indistinguishable $CD4^+$T cells, shown in *Figure 20*.

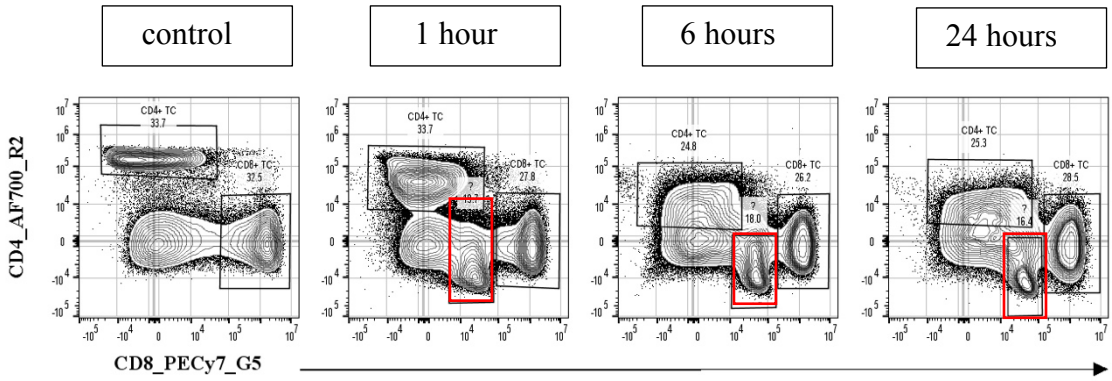

Figure 15. Gating strategy for the analysis of CD4$^+$ lymphocytes in the samples with internalization. *The dot plot shows a sample of isolated lymphocytes, which were activated by PMA/ionomycin. CD4 and CD8 expression were measure at four time points. As control in the beginning, before any manipulation, 1 hour, 6 hours and 24 hours after activation. As becomes apparent CD4 positivity is no longer distinct after 6 hours of activation with PMA/ionomycin. The MFI for CD4 signal decreases as the stimulation progresses. The MFI values for CD8 positivity remain stable throughout the activation.*

Additionally, in samples where I observed internalization, a small population became apparent, which was not present in the non-stimulated blood, highlighted in red frame in *Figure 15*. I tried to identify the properties of the mentioned unknown population.

I created an overlay of dot plots for the unknown population from individual activation time points. I determined that the population remained in the same position. Next, I visualized the unknown population from all time points in the form of multiple histograms to see positivity of each population for degranulation markers CD63 (B4) and CD107a (R3). The unknown population was positive for CD63 (B4 channel) and CD107a (R3 channel). Therefore, I determined that the population was platelets.

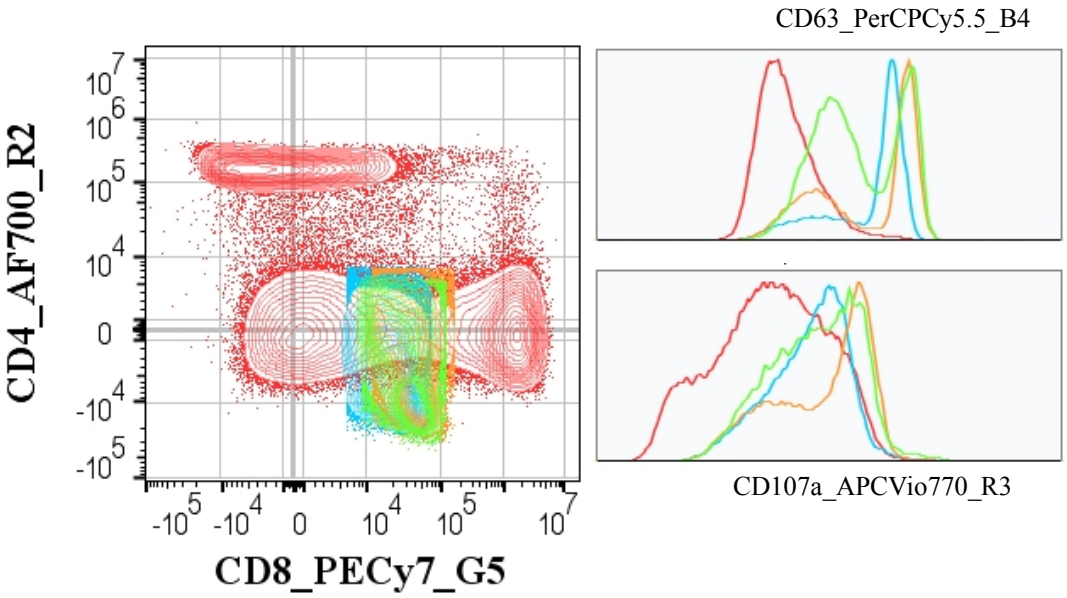

Figure 16. Identification of an unknown population. *Overlaying dot-plots of all cells from non-stimulated blood sample (background) with the unknown population (blue, 1 hour after activation, light green 6 hours after activation, orange 24 hours after activation) appearing during activation parallel with internalization of CD4 marker. Overlaying histograms show positivity of the unknown population for early degranulation markers CD63 (B4) and CD107a (R3).*

Since platelets degranulate excessively there was a strong need to exclude them from the analysis. I experimented with two methods to get rid of the unwanted platelets. First option is based on staining of the sample with CD41 antibody, a platelet marker, shown in *Figure 17*. Second option was based on the centirfugation of PBMC prior to stimulation at 80xg for 20 minutes. Lymphocytes were collected on the bottom of the tube and the platelets remained floating in the supernatant, which led to platelets being discarded with the supernatant before activation. In cytokine detection experiment I decided to get rid of platelets by centrifugation.

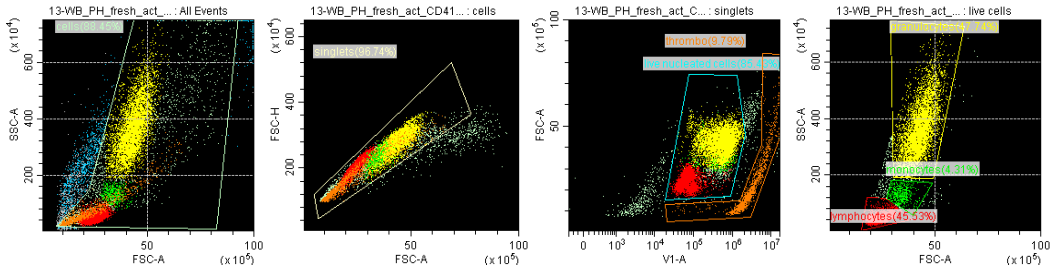

Figure 17 ***Gating strategy to exclude platelets.*** *Staining with CD41_PB, shown in the third graph distinguishes the population of platelets clearly from the rest of PBMC. The resulting blood profile, shown in the last graph is much clearer with separated populations compared to the first one, which depicts the typical profile of platelets across lymphocyte and monocyte populations.*

5.2.2. Detection of degranulation

The first detectable sign of successful activation of PBMC is degranulation. Degranulation markers are detectable after 1 hour of activation. There are two degranulation markers included in the TAT panel, CD63 and CD107a. To evaluate the measured frequencies of antigen-specific T cells, positive controls must be established to compare to the reference frequencies. I stimulated PBMC with polyclonal stimulation in the form of PMA/ionomycin.

After 1 hour of polyclonal stimulation with PMA/ionomycin, neutrophils and monocytes expressed both CD63 and CD107a, while lymphocytes expressed only CD107a. Histograms shown in *Figure 18* were created based on values of Mean fluorescent intensity (MFI) for negative controls and PMA/ionomycin stimulated granulocytes, lymphocytes and monocytes shown in *Table 7*.

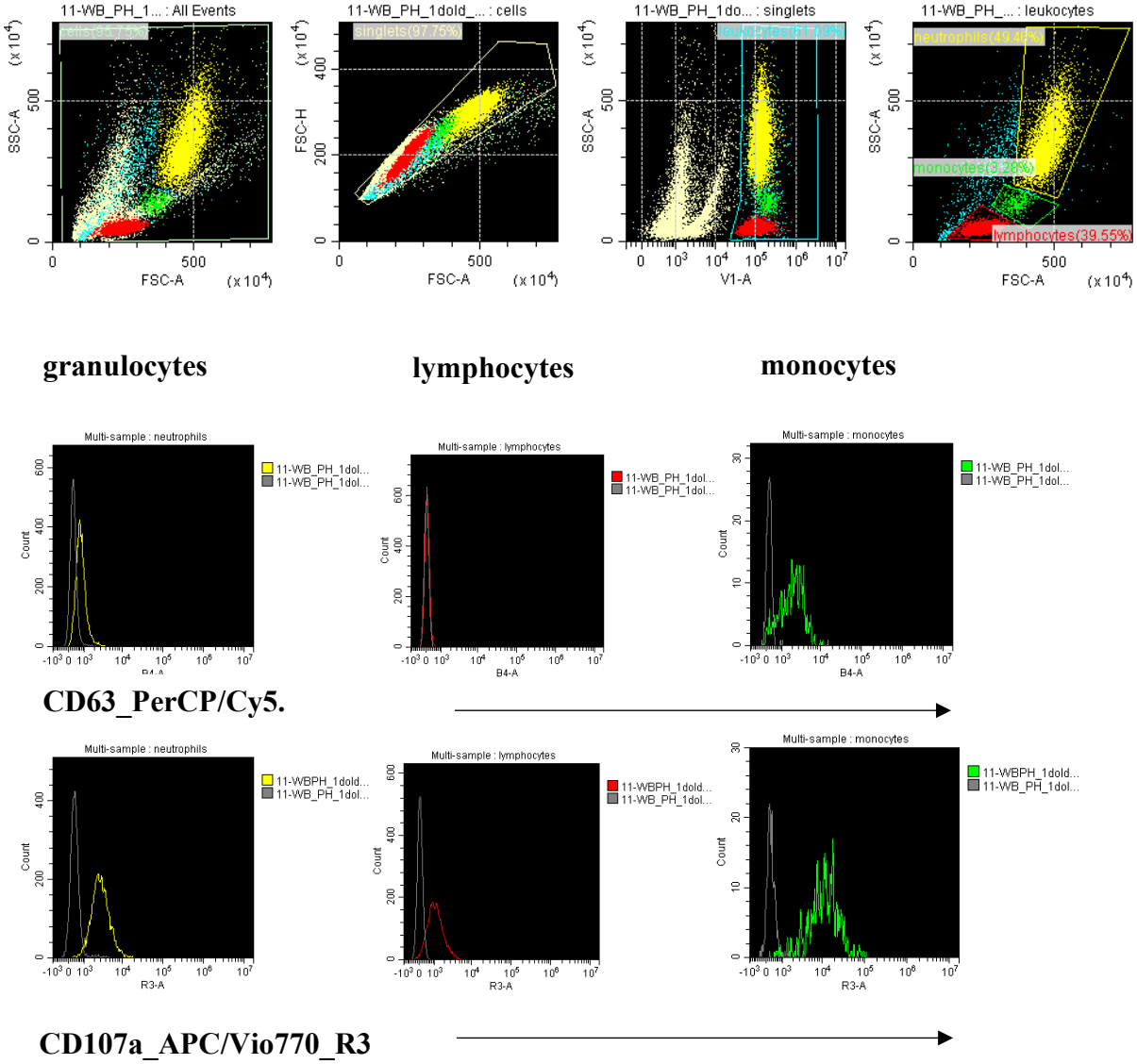

Figure 18. Expression of early degranulation markers CD63 a CD107a on neutrophils (yellow), lymphocytes (red) and monocytes (green). *The first line of graphs shows gating strategy for the clear identification of analyzed populations. The individual graphs demonstrate differences in expression of CD63 and CD107a by individual cell types after 1-hour stimulation with PMA/ionomycin. The grey represents a negative control, cells which were also activated but not stained with the respective antibodies.*

Table 7. ***MFI values for CD63 and CD107a.*** *The MFI values which were obtained from histograms, shown in Figure 18.*

MFI	1h PMA/ionomycin		0h non-activated	
	CD107a	CD63	CD107a	CD63
granulocytes	4 034	846	456	300
lymphocytes	1 829	98	45	30
monocytes	16 132	2 261	174	293

5.2.3. Detection of T cell-specific activation markers

To prove that the PMA/ionomycin stimulation serves as a suitable positive control for detection of T-cell specific early and late activation markers, I included T cell-specific early activation marker CD69 and two late activation markers CD137 and CD154. All three markers are surface markers. CD69 is expressed early, 1 to 6 hours after stimulation. CD137 and CD154 are expressed later, 6 to 24 hours after activation.

CD69 was included in the TAT panel and measured in B1 channel. As shown in *Figure 19 and Figure 20,* over 96% of both $CD8^+$ and $CD8^-$ T cells were successfully activated after 6 hours of polyclonal stimulation with PMA/ionomycin.

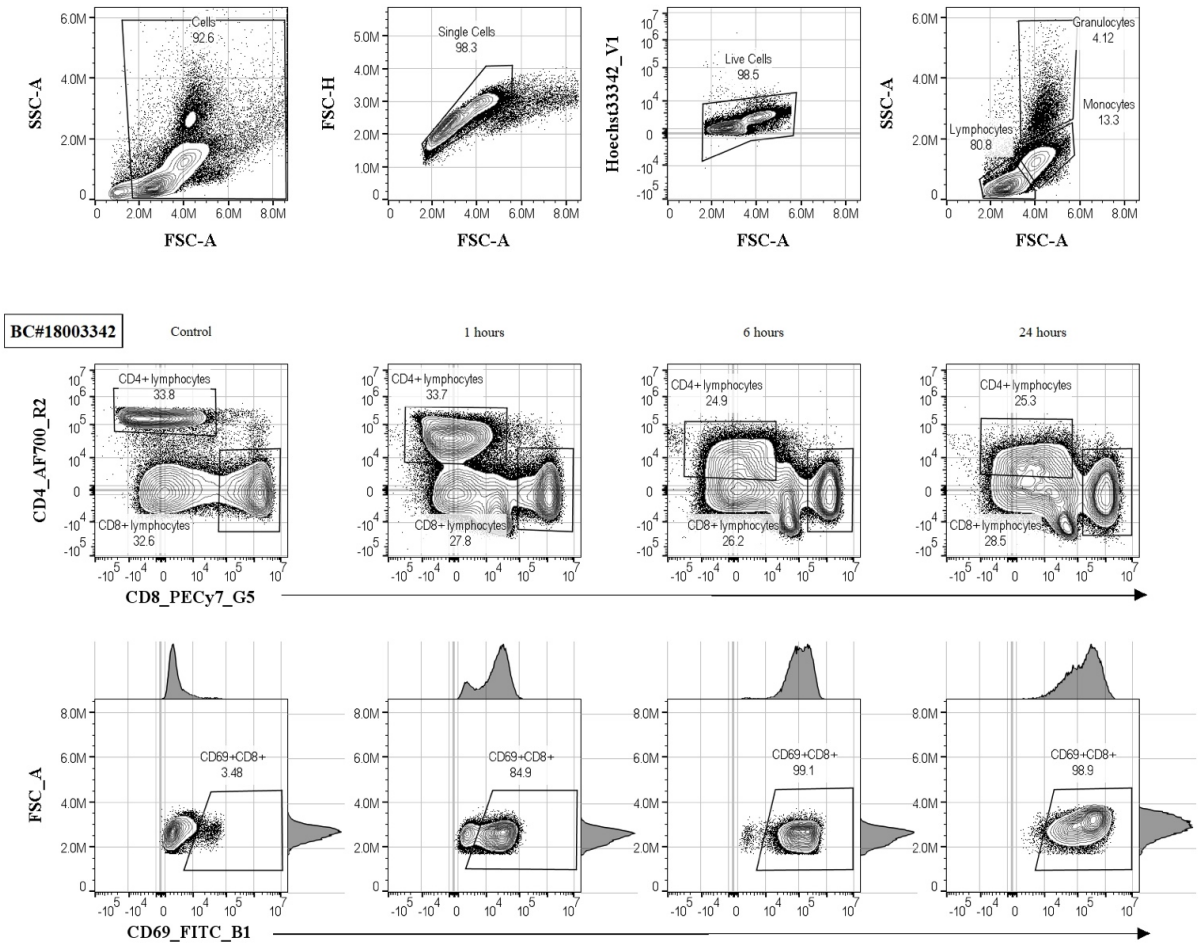

Figure 19. CD69 expression on CD8+ T cells as a positive control of activation of positive control using PMA/ionomycin. *The expression of CD69 marker was measured at 4 time points (initial, pre-stimulation, 1 hour, 6hours and 24 hours after initial stimulation) to monitor the progress of activation in positive controls. CD69 positivity is detected in >99% of CD8$^-$ lymphocytes after 6 hours of activation. The first line of dot plots represents the gating strategy.*

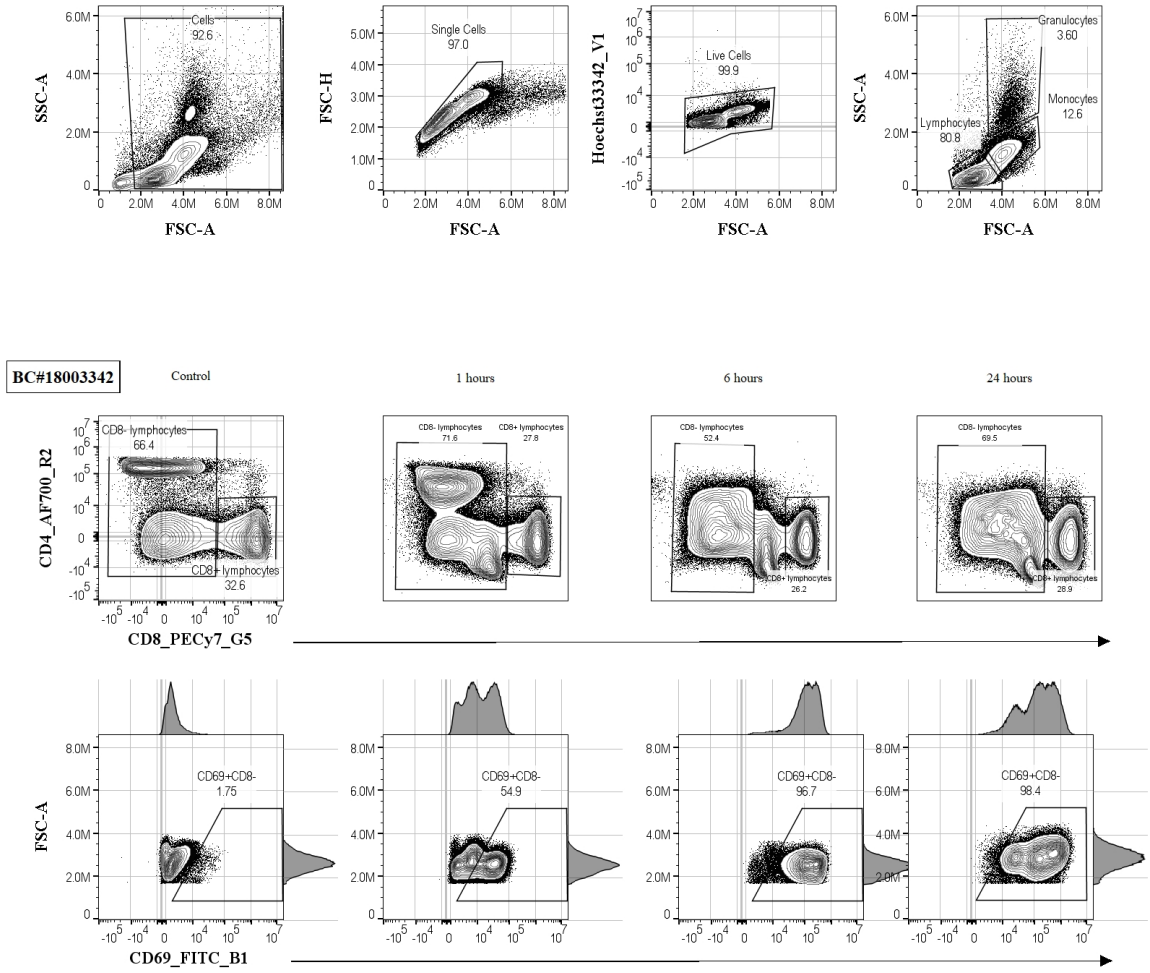

Figure 20. CD69 expression on CD8$^-$ T cells as a positive control of activation of positive control using PMA/ionomycin. *The expression of CD69 marker was measured at 4 time points (initial, pre-stimulation, 1 hour, 6hours and 24 hours after initial stimulation) to monitor the progress of activation in positive controls. CD69 positivity is detected in >96% of CD8$^-$ lymphocytes after 6 hours of activation. The first line of dot plots represents the gating strategy.*

CD137 was measured in V4 channel, data for CD137 positivity are shown in *Figure 21* (CD8$^+$ T cells) and *Figure 22* (CD8$^-$ T cells). CD154 was measured in G1 channel, data for CD154 are shown in *Figure 23* (CD8$^+$ T cells) and *Figure 24* (CD8$^-$ T cells).

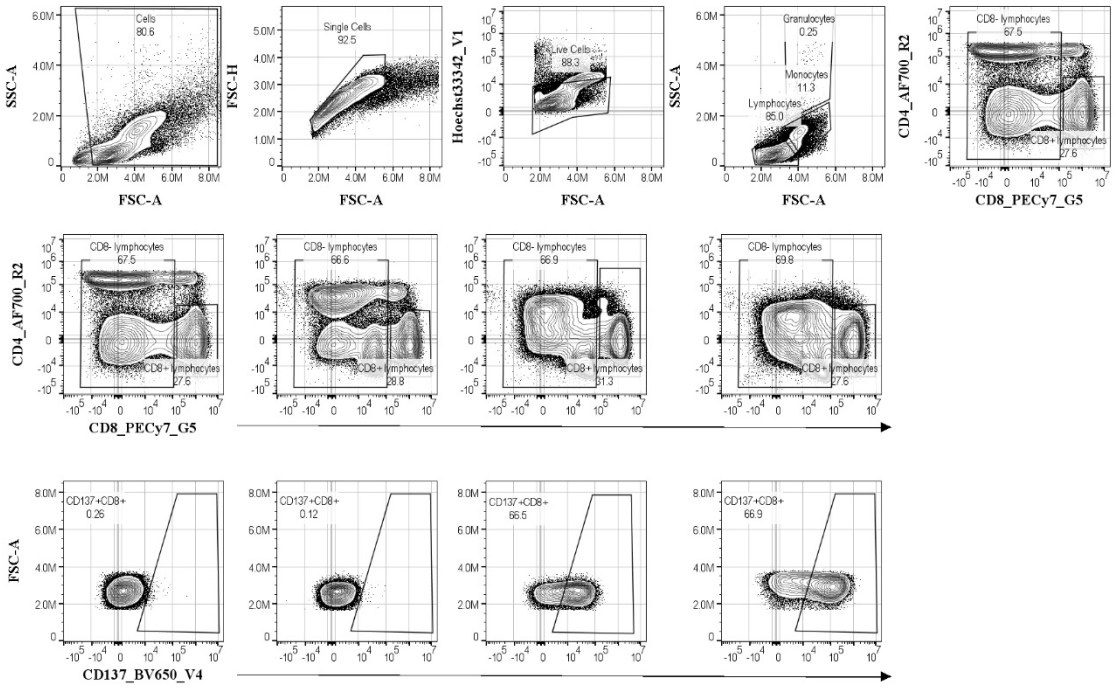

Figure 21. CD137 expression on CD8$^+$ T cells stimulation with PMA/ionomycin. *Figure 19 illustrates the expression of CD137 after stimulation with PMA/ionomycin at 4 time points, (0 hour pre-stimulation, 1 hour, 6hours and 24 hours after stimulation) to monitor the progress of activation in positive controls. The first line of graphs represents the gating strategy.*

CD137 was expressed on 66.5% of CD8$^+$ T cells after 6 hours of stimulation with PMA/ionomycin and was further detected on 66.9% 24 hours post-stimulation.

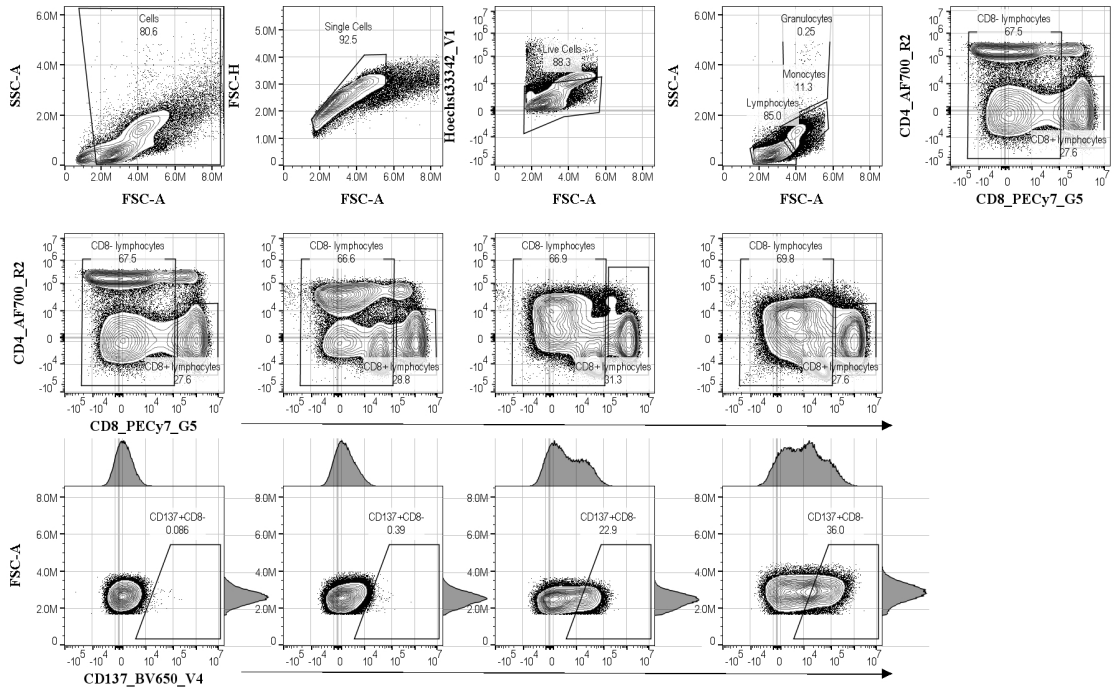

Figure 22. CD137 expression on CD8- T cells stimulation with PMA/ionomycin. *Figure 22 illustrates the expression of CD137 after stimulation with PMA/ionomycin at 4 time points, (0 hour pre-stimulation, 1 hour, 6hours and 24 hours after stimulation) to monitor the progress of activation in positive controls. The first line of dot plots represents the gating strategy.*

CD137 was expressed on 22.9% of CD8- T cells after 6 hours of stimulation with PMA/ionomycin. After 24 hours of stimulation, 36% of CD8- T cells were positive for CD137.

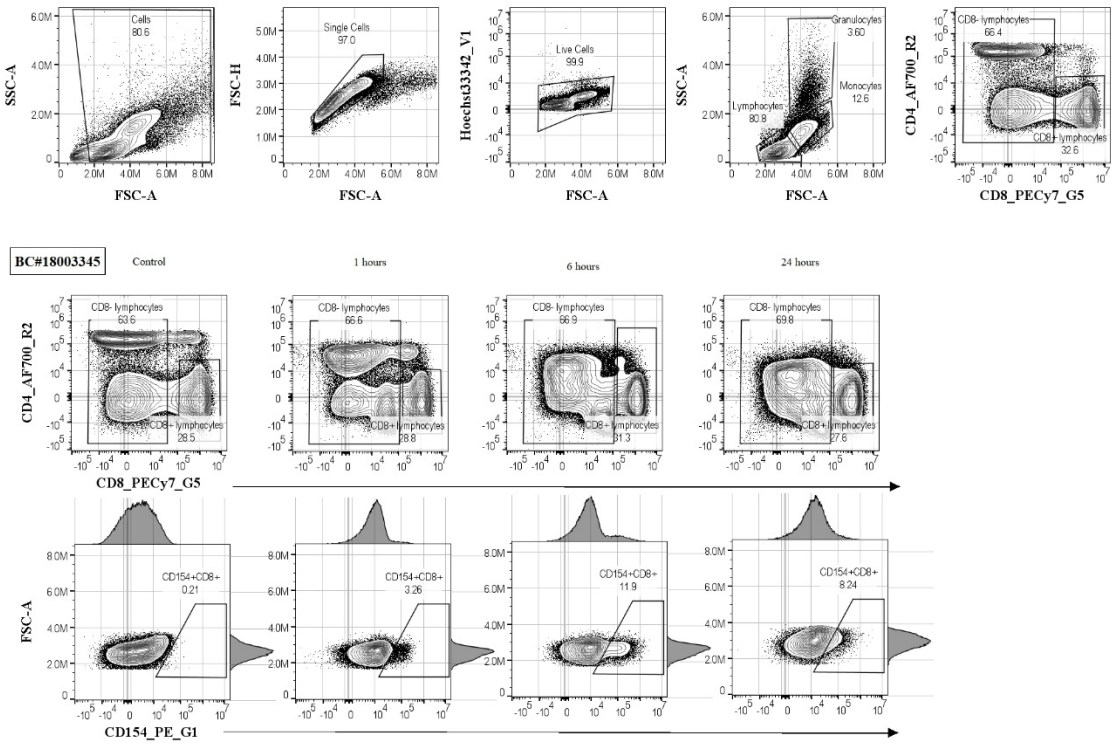

Figure 23. ***CD154 expression on CD8$^+$ T cells stimulation with PMA/ionomycin.*** *Figure 22 illustrates the expression of CD154 after stimulation with PMA/ionomycin at 4 time points, (initial, pre-stimulation, 1 hour, 6hours and 24 hours after initial stimulation) to monitor the progress of activation in positive controls. The first line of graphs represents the gating strategy.*

Expression of CD154 on CD8$^+$ T cells was detected 1 hour after stimulation at 3.26%, the expression increased to 11.9% after 6 hours of stimulation and decreased again to 8.24% 24 hours after stimulation.

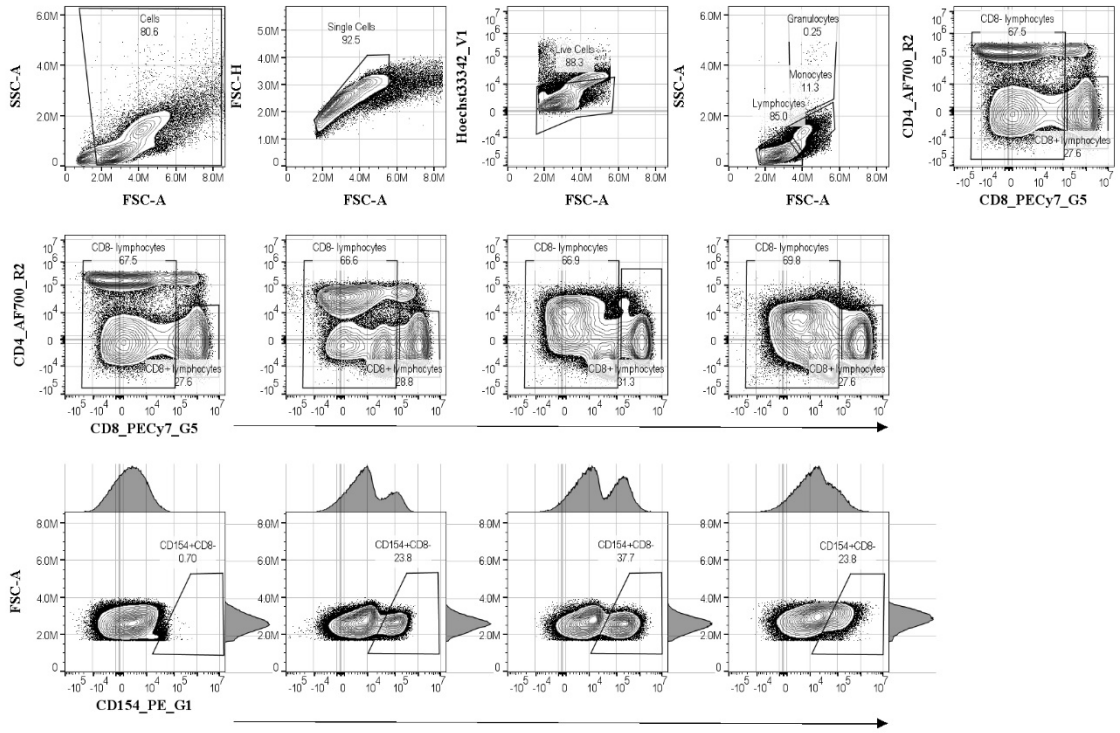

Figure 24. ***CD154 expression on CD8- T cells stimulation with PMA/ionomycin.*** *Figure 21 illustrates the expression of CD154 after stimulation with PMA/ionomycin at 4 time points, (time 0, 1 hour, 6hours and 24 hours after stimulation) to monitor the progress of activation in positive controls. The first line of dot plots represents the gating strategy.*

Expression of CD154 on $CD8^-$ T cells was detected 1 hour after stimulation at 23.8%, the expression increased to 37.7% after 6 hours of stimulation and decreased again to 23.8% 24 hours after stimulation.

Measured signal for CD69, CD137 and CD154 on $CD8^+$ and $CD8^-$ T cells proved that polyclonal stimulation with PMA/ionomycin serves as a suitable positive control for the TAT panel.

5.3. Cytokine detection

Cytokines are intracellular markers of T cell activation. Since the monitoring methods used in BCa treatment, LTBI diagnosis and monitoring are frequently based on cytokine release detection, I decided to include three major cytokines in the TAT panel. They are IL-2, TNFα and IFNγ. To confirm its functionality as a positive control I stimulated the cells with PMA/ionomycin.

I also activated T cells using another polyclonal stimulus, PHA to serve as an additional positive control for the final TAT. PHA is beneficial because in contrast to PMA/ionomycin it does not lead to CD4 internalization, which enables more accurate phenotyping of activated T cell subsets. I stimulated PBMC isolated from buffy coats from three donors, BC#18005433, BC# 18005434, BC# 18005439.

During the microscopy control of activation progress, I detected that the PMA/ionomycin stimulation showed abnormalities. During measurement the PMA/ionomycin activation proved faulty, which led me to discard it from analysis and focus solely on PHA stimulation as a positive control.

The first measured cytokine was TNFα, shown in *Figure 23*. I measured TNFα positivity on $CD4^+$ and $CD4^-$ T cells because I detected no signal, when gating on $CD8^+$ T cells.

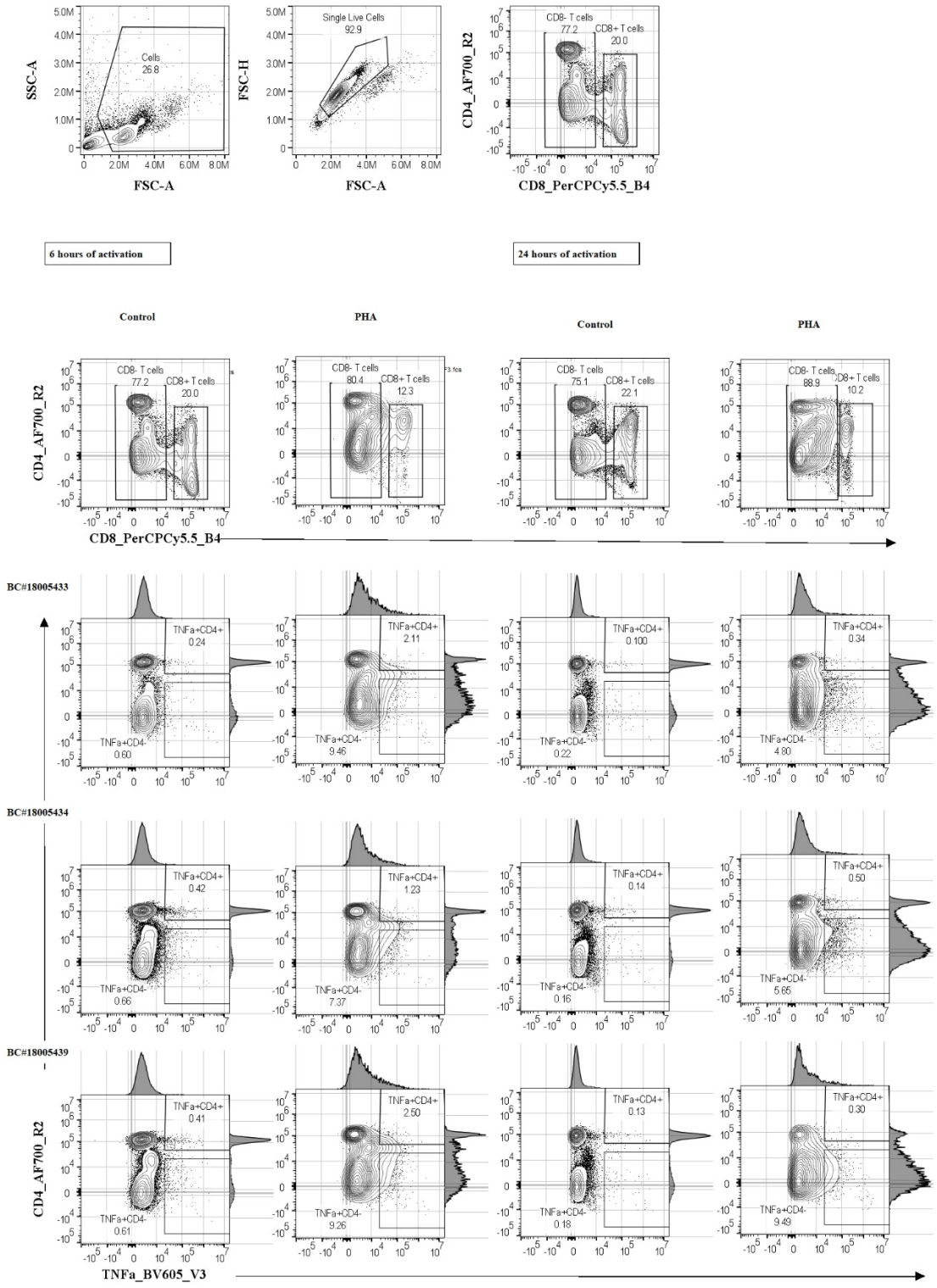

Figure 25. Detection of TNFα on CD4⁺ and CD4⁻ T cells. *TNFα was measured after stimulation with PHA on subsets of CD4⁺ and CD4⁻ T cells 6 hours and 24 hours after initial stimulation. Each row represents one donor, BC#18005433, #18005434 and #18005439. Dot plots in the first row show gating strategy for the analysis.*

After polyclonal stimulation with PHA I was able to detect expression of TNFα on both $CD4^+$ and $CD4^-$ T cells. 6 hours after activation with PHA, the positivity for $CD4^+$ T cells ranged between 1.23% and 2.50% and it decreased to 0.30%-0.50% after 24 hours, which was at the level of negative controls. For $CD4^-$ T cells positivity ranged between 7.37% and 9.46% after 6 hours of stimulation with PHA and stagnated or decreased to a range between 4.80% and 9.49% after 24 hours of stimulation.

Second cytokine included in the TAT was IL-2. IL-2 is a major T cell cytokine, which indicates T cell activation. I detected signal only for $CD4^+$ T cell subset.

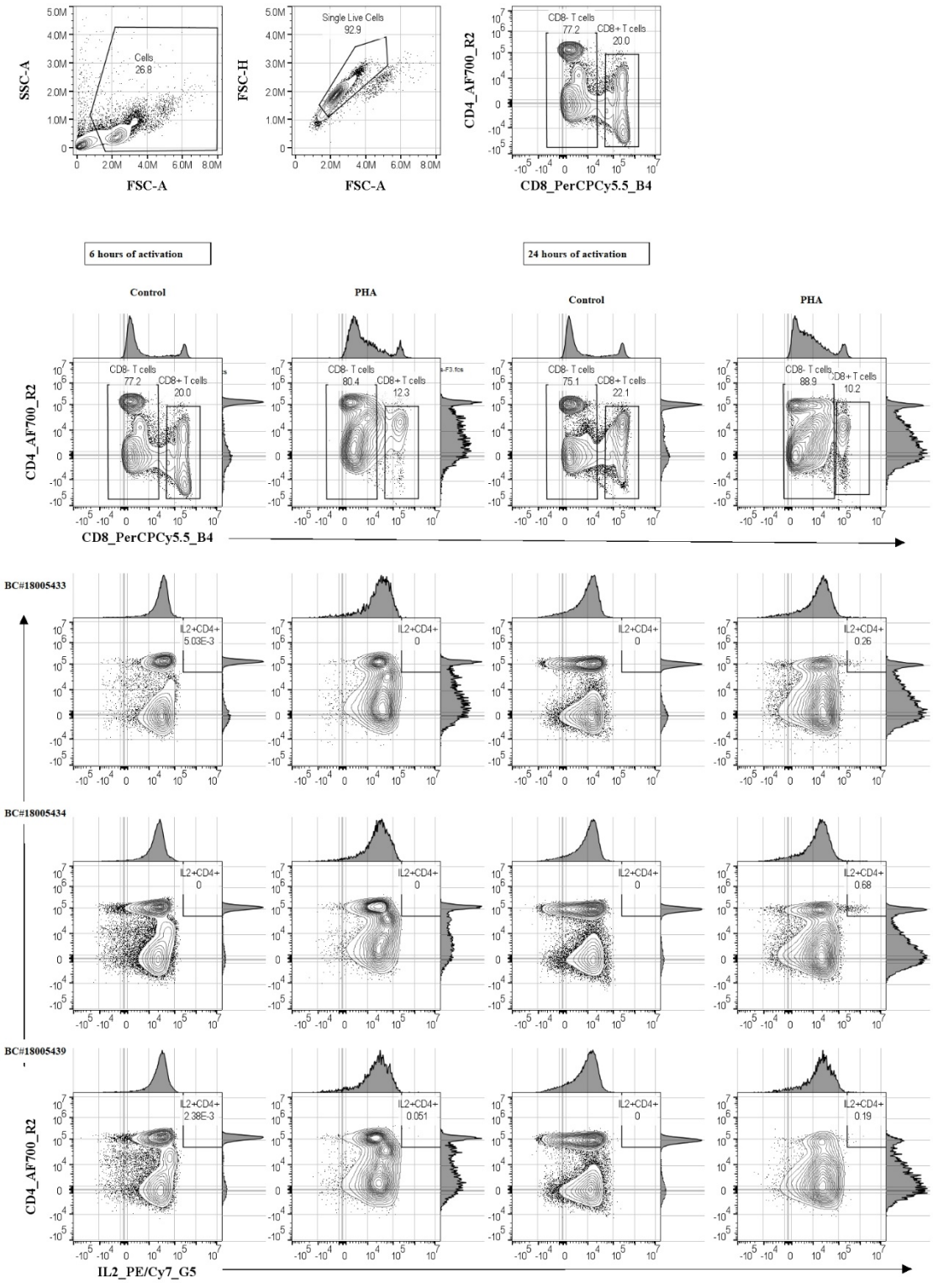

Figure 26. Detection of IL2 on CD4$^+$ and CD4$^-$ T cells. *IL2 was measured after stimulation with PHA on subsets of CD4$^+$ and CD4$^-$ T cells 6 hours and 24 hours after initial stimulation. Each row represents one donor, BC#18005433, #18005434 and #18005439. The first row depicts gating strategy for the analysis.*

IL2 expression was detected only after 24 hours from initial stimulation on a subset of 0.19% to 0.68% of $CD4^+$ T cells with no detectable signal after 6 hours. There was no expression of IL2 on $CD4^-$ T cells at either time point.

5.4. CMV-specific response

CMV stimulation serves as a control of antigen-specific T cell response for the TAT. It was selected as a positive control because CMV-specific T cells are more frequent than the expected frequencies of BCG-specific and tumor-specific reactive T cells and because of high number of positive donors in the population.

PMA/ionomycin and PHA stimulation served as positive controls for the CMV stimulation. I measured surface activation markers after CMV stimulation. To enhance the CMV-positive response I measured their expression after re-stimulation. The acquired data are shown in *Figure 27*.

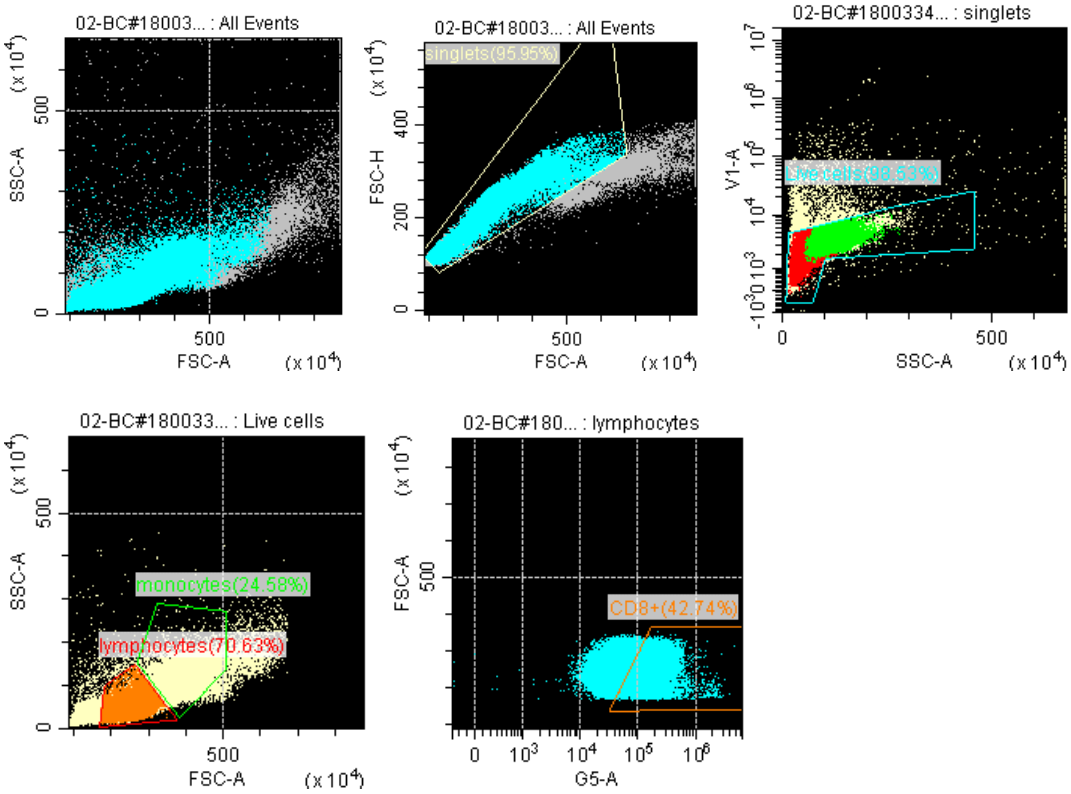

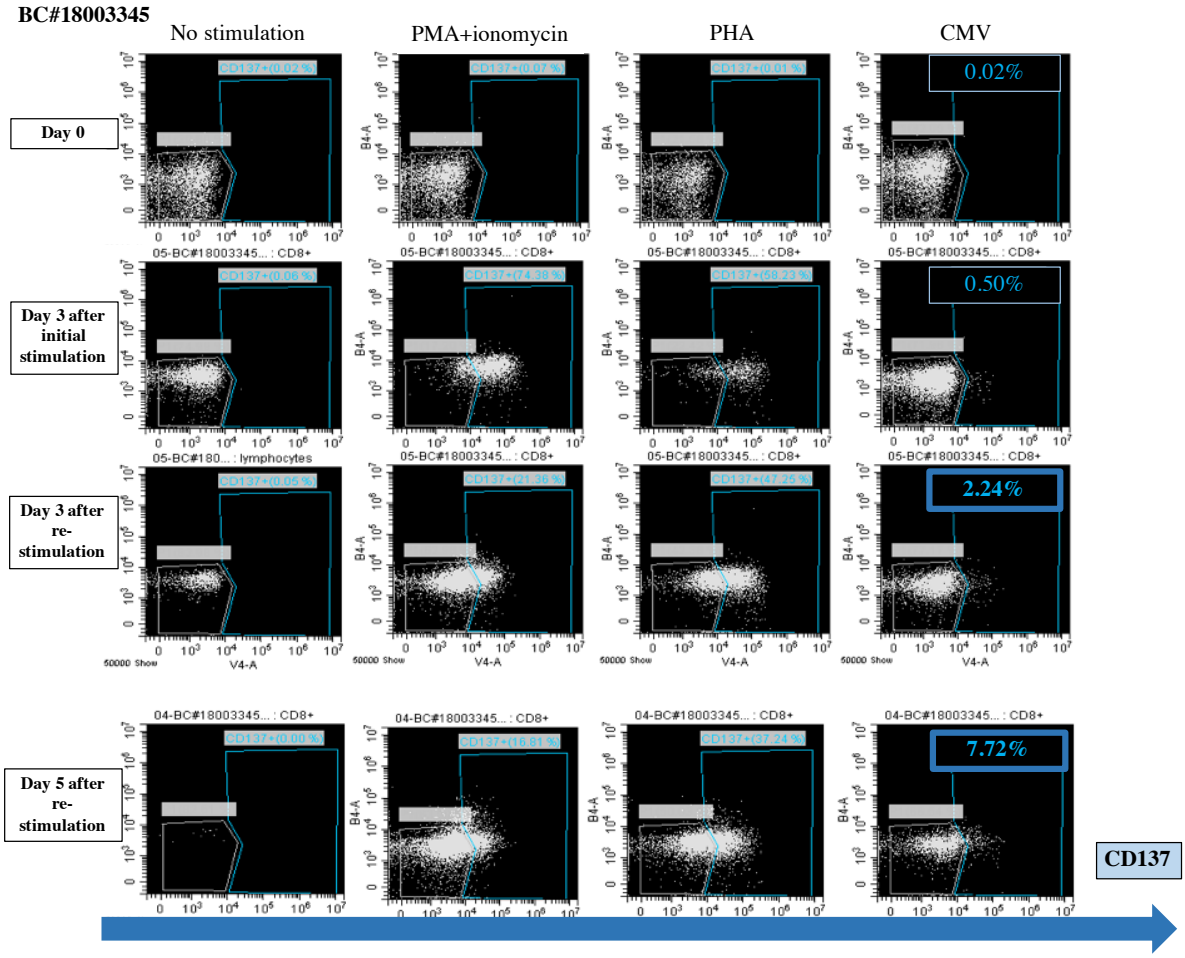

Figure 27. Detection of low frequency CD8$^+$ T cell populations of a single donor in response to CMV stimulation at different time points. *The responsive CD8+ T cells were detected based on expression of late activation surface marker CD137 (V4-A) on BC CytoFLEX S cytometer. Expression of CD137 was measured 5-days post-stimulation with CMV lysate in comparison to non-stimulated control and positive control stimulated with PMA/ionomycin and PHA. On day 7, PBMC were re-stimulated and the expression of CD137 was measured 3- and 5-days post re-stimulation.*

As the *Figure 27* illustrates, using flow cytometry, I was able to identify a rare CMV-responsive population of CD8+ T cells based on the expression of late surface activation marker CD137. Specific activation is apparent from the 3rd day after initial stimulation, when I observed a population of 0.50% of CD8+ T cells, which were responsive to CMV stimulation. The frequency of reactive CD8+ T cells increased up to 7.72% of CMV-responsive CD8+ T cells 5 days after re-stimulation with CMV.

5.5. UniCAR

As another antigen-specific positive control I proposed a spike experiment using the uniCAR T cell system. I used the PSCA as the positive control. PSCA is the target antigen present on the surface of prostate cancer cell lines PC-3 and LNCap. I included PSCA because it is also frequently expressed on BCa cells.

First, I proved the expression of PSCA on LNCap prostate cancer cell line by performing SDS-PAGE gel, shown in *Figure 28*.

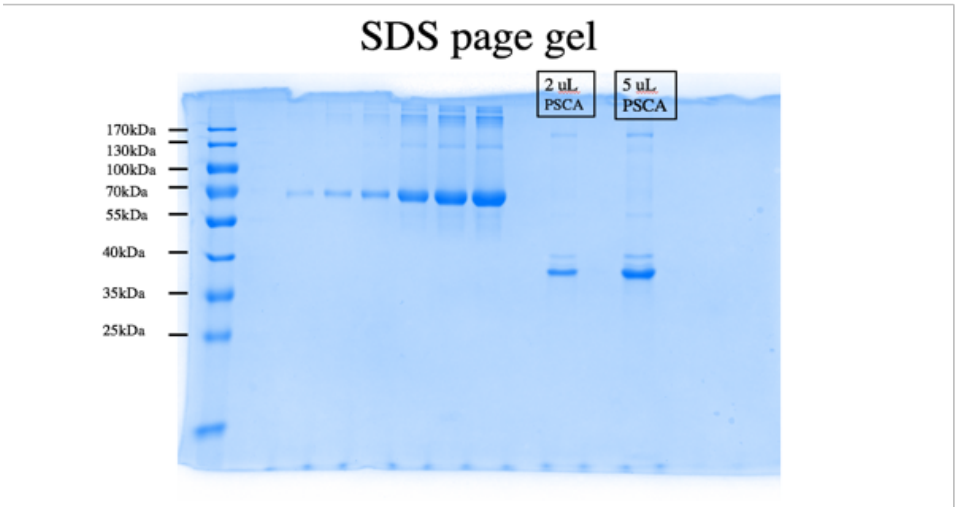

Figure 28. SDS-PAGE gel to prove presence of PSCA on LNCap cell line. *PSCA expression was proved on LNCap prostate cancer cell line.*

TM binding to the cancer cell line is prerequisite to the interaction between uniCAR T cell and the tumor cell, which leads to tumor cell eradication. I ran a Western Blot, *Figure 29* to prove the presence of the desired TM.

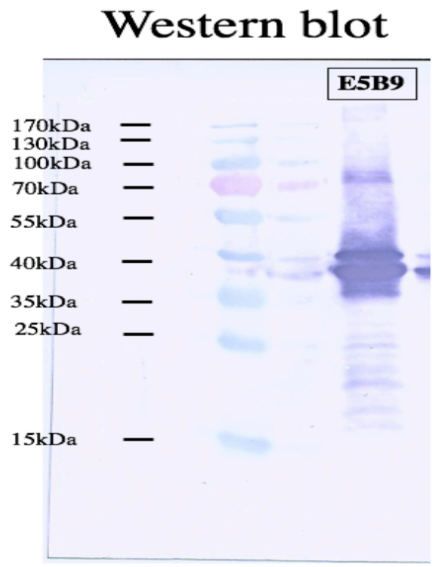

Figure 29. Western Blot. *The Western Blot was used to prove the binding of the TM with E5B9 epitope to LNCap. The E5B9 was detected via a specific antibody and a secondary GAM-HRP…*

Finally, I collected data on positive results proving the antigen-specific binding by the uniCAR system, which might serve as another potential positive control, detecting its functionality through a binding assay, see *Figure 30*.

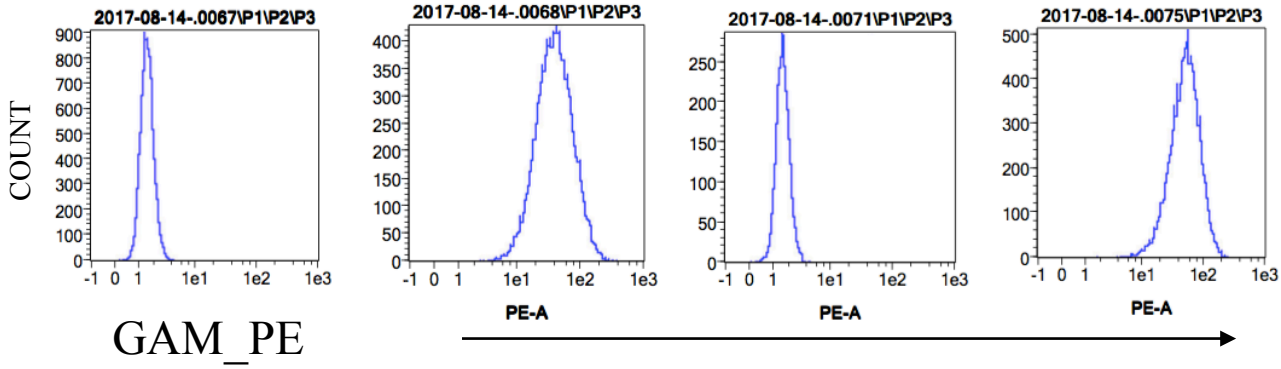

Figure 30. Binding assay*. The binding assay is a proof of the interaction between the uniCAR T cells and the tumor cells. The first and third graph are negative controls for PC-3 and LNCap cell lines, respectively. The negative controls were prepared by adding the secondary antibody (GAM_PE) to the cells without TM. The second and fourth graphs show positive controls, both TM and secondary antibodies were added to the uniCAR T cells and tumor cells.*

I did not use the transduced uniCAR T cells for the positive control spike experiment because the process of preparation results in limited yields of transduced cells. The team in German laboratory could not spare the necessary transduced cells before the completion of my diploma project due to their own ongoing research. Nonetheless, uniCAR T cells can be used as positive control to be stimulated by selected TM or a combination of TMs suitable for BCa and/or LTBI and other pathologies not limited to PSCA. I will attempt to acquire the necessary materials to exploit the uniCAR T cells as positive control in the near future.

Despite my mistake in handling CD8 antibody, the split of the panels proved practical for handling the donor samples in preparation for staining as well as in terms of time management of activation and collection of cells from culture where they were exposed to stimulants. Second major advantage of the split was in making the calculation of compensation easier and more manageable in the terms of manual adjustment of the compensation matrix to achieve.

I tested degranulation markers CD63 and CD107a, surface markers CD69, CD137 and CD154 and cytokines IL-2, IFNγ and TNFα on positive controls using PMA/ionomycin and PHA stimulants. I was able to detect positivity for all markers except for IFNγ. The conducted tests proved that PMA/ionomycin and PHA are suitable positive controls.

I was further able to detect CMV-specific T cell response on CD137 activation marker. This result shows that CMV is a suitable candidate for positive control of antigen-specific T cell response. However, the CMV stimulation requires more testing as well as the uniCAR T cell system.

6. Discussion

I designed a 10-parametric TAT panel, *Table 4* for potential use in the BCG therapy targeting BCa and LTBI. Combination of markers proves more efficient in immune response monitoring than narrowly focused panels. Therefore, the TAT panel included T cell core markers, degranulation markers, surface activation markers and cytokines. A similar multiparametric panel has been proposed for the use in monitoring patients' response to immunotherapy by mass cytometry including markers from across the spectrum, covering early and late surface markers, cytokines, degranulation markers and markers of different cell types[130].

Because of a mistake I made when titrating CD8_PO antibody I was not able to test the complete panel on my positive controls. Since I could not afford to purchase new CD8_PO antibody, I had to design alternative panels. The complete TAT panel was divided into two, one for the surface markers (CD4, CD8, CD63, CD107a, CD69, CD137 and CD154), *Table 5* and the second one for intracellular staining (CD3, CD4, CD8, IL-2, IFN-γ and TNF-α), *Table 6*. The two panels remain compatible and may be unified into one again.

The split of the panel proved quite practical because it was easier to set up, calculate and apply compensation, which was performed on VersaComp beads for both surface markers and cytokine detection panels. Because of high gains (maximum=3000) in the red and far red spectrum (G5, R1, R2, R3 channels), listed in *Table 4* and demonstrated on Rainbow beads in *Figure 5*, the values in compensation matrix are also high leading to higher spread in the negative populations. Despite that, an orthogonal distribution among individual populations was achieved for the cytokine detection panel (6 parameters), *Figure 11*. In the larger panel for surface markers (8 parameters) I was not able to achieve orthogonality among all channels despite manual adjustment of the compensation matrix, *Figure 10*. There was a non-orthogonal distribution between B4 (CD63) and R2 (CD4) and between G5 (CD8) and R3 (CD107a). The same suboptimal compensation was proved by visualization of spillover in *Figure 12*.

I observed a high background signal in the cytokine detection panel, especially in V3 (TNFα), G1 (CD3) and R1 (IFNγ), *Figure 12*. Despite the above discussed issues, I

conclude that I was able to compensate the panels sufficiently and both were suitable for further testing to establish positive controls for the final TAT.

To accurately analyse T cell specific response, first I analysed detected positivity for included T cell core markers CD3, CD4 and CD8 in all included donors in non-stimulated PBMC. CD8 marker was expressed steadily with a population of 17.7%-28.5%, exemplary sample shown in *Figure 15*. CD8 was stably expressed and detectable in each donor. CD8 counts are in accordance with the published reference numbers for Caucasian population[131].

To test the functionality of the designed TAT panel and select the optimal positive controls for the TAT, I experimented with polyclonal (PMA/ionomycin, PHA) and antigen-specific (CMV lysate) stimulation.

First, I analysed the data collected on T cell core markers to ensure analysis of T cell-specific response. I measured the expression of CD4 and CD8 markers on non-stimulated blood, *Figure 14*. Then I observed the kinetics of T cell core markers, to confirm stability of expression, *Figure 15*. I determined, that CD4 marker internalized after stimulation with PMA/ionomycin. The beginning of downregulation of CD4 markers was observed already at 1 hour after activation, *Figure 15* and *Figure 24*. However, when stimulated by PHA and CMV I did not observe any CD4 downregulation, *Figure 25*. The phenomenon of CD4 internalization after stimulation with PMA/ionomycin was described in literature[132].

The downregulation complicates the analysis of reactive $CD4^+$ T cells. For the purposes of phenotyping of $CD4^+$T cells or in case I am particularly interested in the $CD4^+$ T cell-specific response, a PHA will be a better positive control. Alternatively, $CD4^+$ T cells can be included in the analysis by setting a wide gate on $CD8^-$ T cell population, *Figure 20, Figure 22* and *Figure 24* or by gating more accurately on $CD3^+CD8^-$ T cells. So far, I have not tried gating on $CD3^+CD8^-$ T cells and I have analysed $CD8^+$ and $CD8^-$ T cell population[133].

As shown in *Figure 15*, I detected an unknown population during the activation process. In order to identify the origin of the population I gated on the population at each time point, 1 hour, 6 hours and 24 hours after stimulation. I followed an analysis strategy described in the Results and by overlaying the populations on a dot-plot, *Figure 16* and looking at the

positivity for CD63 and CD107a degranulation markers I determined that it was a population of platelets. Since platelets degranulate, aggregate and express activation markers including CD154[95] they interfere in the data analysis Therefore, I needed to exclude them from the measurement. As shown in *Figure 17*, platelets can be easily and precisely excluded by staining the sample with CD41 platelet marker[124]. Another possibility how to exclude platelets is to centrifuge the sample at 80xg for 20 minutes before activation. Data collected on cells activated after PBMC were centrifuged and platelets were discarded with the supernatant used for cytokine detection, *Figure 25 and 26*.

I decided to always use the centrifugation to get rid of platelets in the TAT for two reasons. The first one is that adding an unnecessary antibody into a 10-parametric TAT panel results in more error-prone analysis. Additionally, I used CD41_PB, which is detected in V1 channel that I need to keep free for a viability dye. The second reason is that those platelets, which are adherent and have aggregated on lymphocytes, will be excluded from the analysis, due to CD41 positivity. The second reason is simply practical. Centrifugation is cheaper and faster than an additional staining step.

After I made sure that I was truly analysing T cells, I moved on to analysis of the earliest activation markers, degranulation markers. The expression of early degranulation markers CD63 and CD107a was clearly detectable after 1 hour of stimulation. There was a clear pattern of expression of each marker based on the observed cell type. The positivity was analysed based on changes in the MFI value, listed in *Table 7*. As shown in *Figure 18*, CD63 was clearly detected on monocytes (MFI from 293 on negative control to 2261 on activated cells) and granulocytes (MFI from 300 on negative control to 846 on activated cells). CD63 was not expressed on lymphocytes (MFI from 30 to 98). CD107a expression was detected on monocytes, granulocytes and lymphocytes. These observations prove that stimulation was successful and are in accordance with the published data[134,135]. Since the MFI increased significantly in the positive controls I conclude that including the detection of degranulation is a useful asset to the TAT panel.

The next step in the activation cascade is detection of early, T cell specific activation marker, CD69. Since I tested the positivity for all the remaining surface markers CD69, CD137 and CD154 on PBMC stimulated with PMA/ionomycin, I was only able to

determined the positivity on $CD8^+$ and $CD8^-$ T cells but not more accurately on $CD4^+$ T cells for the reasons stated above. I detected CD69 positivity in over 99% of $CD8^+$ T cells, *Figure 19* and in over 96% if the $CD8^-$ T cells, *Figure 20* stimulated with PMA/ionomycin. In published work, CD69 positive population represented 93% of all T cells[136] and was used for detection of T cell activation after polyclonal and oligoclonal stimuli[137], which is the case for my results as well. Therefore, CD69 is a valid marker for the TAT panel and PMA/ionomycin is a suitable positive control to detect it.

Regarding the late activation surface markers, CD137 and CD154 are the two included in the TAT panel. I tested CD137 positivity on PBMC stimulated with PMA/ionomycin, which was proved to work in published work[138]. CD137 was detectable in 66.5% of $CD8^+$ T cells and in 22.9% of $CD8^-$ T cells after 6 hours and in 66.9% of $CD8^+$ T cells and 36% of $CD8^-$ T cells after 24 hours of stimulation. Data are shown in *Figure 21* and *Figure 22* for $CD8^+$ T cells and $CD8^-$ T cells respectively.

I detected CD154 positivity after polyclonal stimulation in both $CD8^+$, (*Figure 23)* and $CD8^-$ T cells, (*Figure 24)* but the population of $CD154^+$ cells was higher 37.7% at 6 hours after stimulation for $CD8^-$ T cells compared to 11.9% at 6 hours after stimulation for $CD8^+$ T cells. $CD154^+$ has been reported to be detected on a population of $CD4^+$ T cells[113], which I was able to confirm with my results.

After establishing positivity on the surface markers, I experimented with the cytokine panel. Originally, I activated the cells using both polyclonal stimuli as positive controls, PMA/ionomycin and PHA. Due to abnormal and insufficient activation with PMA/ionomycin which I confirmed under a microscope and by measurement. I suspect I used a different batch of ionomycin, which was not stored properly. For the positive stimulation to detect cytokines, I therefore used PHA. I included antibodies against TNFα, IL-2 and IFNγ.

Strongest expression of TNFα was detected 6 hours after activation with PHA, *Figure 25*. The frequency of TNFα positive cells decreased to between 0.30% and 0.50% and 4.80% to 9.49% for $CD4^+$ and $CD4^-$ T cells respectively 24 hours after activation. After PMA ionomycin stimulation the expected positivity for TNFα is above 40%[132]. In the published work, the highest positivity achieved by PHA stimulation was detected after 8 hours of stimulation[139]. The lower percentage of $TNF\alpha^+$ T cells might be caused by suboptimal

conditions of stimulation, which was too short for the activation with PHA as a positive control and suboptimal with PMA/ionomycin.

I detected IL2 expression for $CD4^+$ T cells after 24 hours of stimulation with PHA, *Figure 26*. The positivity ranged between 0.19% and 0.68%. I detected no positivity for neither $CD4^-$ T cells nor for $CD8^+$ T cells. After polyclonal stimulation the expected IL2 positivity is nearly 50%[140]. Since I detected the IL-2 antibody conjugated to PE/Cy7 fluorochrome on beads I ruled out the possibility of any fault with the antibody.

Because of lower than expected expression of TNFα and IL-2 I tried to identify the reason for lower expression. I always confirmed the activation by microscopic observation of the sample at 6 hours and 24 hours of activation. The significantly lower ratio of detected positivity might be caused by suboptimal permeabilization. To prevent a mistake in permeabilization, I included a control by staining a control sample of the same type of cells with intracellular marker. Another reason of the lower positivity may be wrong handling of the antibody, resulting in losing fluorescence.

Expected IFNγ positivity after polyclonal stimulation is 30% [140]. I was not able to detect any IFNγ on either T cell subset even after following the activation protocol for positive controls described in the manufacturer's manual. After CMV stimulation, cytokines were reported to be detectable on $CD4^+$ T cells[113].

Due to contamination I was not able to detect any cytokines on CMV-stimulated cells.

To test a positive control for antigen-specific stimulation, I detected CD137 positivity on PBMC from one healthy donor after 72 hours after stimulation. Significant increase of $CD137^+$ T cells was detectable 3 days after re-stimulation. The strongest signal was measured 5 days after re-stimulation and reached 7.72% of $CD8^+$ T cells*, Figure 27*. In a study focused on CMV status in donors for patients ready for a stem cell transplant, $CD137^+$ positive T cells have been detected at a median of 6.2%, ranging from 0.4 to 26.2%[141], confirming my results.

As part of my ERASMUS+ practical internship, I have been introduced to the establishment, production and testing of uniCAR T cells. I have been able to detect the expression of PSCA antigen on an SDS PAGE gel as expected[44], *Figure 28*. As the next step, I have used confirmed the presence of E5B9 epitope, which is used to mediate

interaction between uniCAR T cells and the tumor cell, *Figure 29*. The expression of E5B9 neoepitope works as an essential part of the binding domain, proving successful construction of the uniCAR domain[44]. The binding assay, *Figure 30* is the last step to prove that the interaction between T cell and tumor cell can occur. This shows that the transformation of the cells and the construction of uniCAR domain has been successful and the system may be taken to be tested in animal models or used for different purposes such as controls for T cell responses[44,142].

UniCAR T cells can be exploited as a positive control for monoclonal stimulation for the most common stimulating antigens. The extracellular domain which I used binds the PSCA (PSCA gene) cell surface marker[143], which has been detected in BCa samples but other epitopes may be designed.

In conclusion the TAT panel is suitable for further testing with the focus on detection of antigen-specific T cell response with polyclonal (PMA/ionomycin, PHA) and antigen-specific (CMV and uniCAR T cells) stimulants as positive controls.

7. Conclusion

In my diploma project I focused on developing a stratification and monitoring method based on flow cytometry detection of antigen-specific T cell response, applicable for BCG based therapies namely for BCa and LTBI patients. My goals were to design a TAT panel suitable for FCM, optimize positive controls for the future use of TAT and test the efficiency of TAT in detecting antigen-specific T cell response.

I successfully designed a 10-parametric panel for FCM. Since I had to split the original complete panel in two, the compensation matrices from CytExpert and FlowJo softwares are only applicable to the respective panels. Nonetheless, the panels stayed compatible and it remains a priority to unify the panels into one and test the originally designed TAT in its entirety on both the polyclonal stimulation as well as for its efficiency in detection of rare antigen-specific T cell populations.

I managed to establish the stimulation of lymphocytes isolated from whole blood of healthy donors with PMA/ionomycin and PHA. PHA allows for more accurate positive control, since it does not lead to internalization of CD4 marker. These stimulations will serve as positive controls for the final TAT. After stimulation with CMV I was also able to detect the antigen-specific T cell population, using the surface activation markers panel. Even though the CMV-responsive T cell populations are more frequent than the expected frequencies of rare tumor- and *M.tuberculosis*-specific T cells, it served to prove the validity of the proposed stratification method.

Unfortunately, I did not have the opportunity to employ uniCAR T cells as positive controls for antigen-specific stimulation due to limited access to the material.

In conclusion, the designed TAT panel has a high potential for application in cases of BCG-based therapies. It will be further tested on T cell populations stimulated by BCG-, *M.tuberculosis*- and tumor-specific antigens.

References

1. *Novotvary 2015 ČR, Cancer Incidence in the Czech Republic, 2015*. (Ústav zdravotnických informací a statistiky ČR, 2015).
2. Cline, M. S. *et al.* Exploring TCGA Pan-Cancer Data at the UCSC Cancer Genomics Browser. *Sci. Rep.* **3**, 2652 (2013).
3. Morales, A., Eidinger, D. & Bruce, A. W. Intracavitary Bacillus Calmette-Guerin in the treatment of superficial bladder tumors. *J. Urol.* **116**, 180–183 (1976).
4. Chamie, K. *et al.* RECURRENCE OF HIGH-RISK BLADDER CANCER: A POPULATION-BASED ANALYSIS. *Cancer* **119**, 3219–3227 (2013).
5. Nadal, R. & Apolo, A. B. Overview of Current and Future Adjuvant Therapy for Muscle-Invasive Urothelial Carcinoma. *Curr. Treat. Options Oncol.* **19**, 36 (2018).
6. Kamat, A. M. *et al.* Predicting Response to Intravesical Bacillus Calmette-Guérin Immunotherapy: Are We There Yet? A Systematic Review. *Eur. Urol.* **73**, 738–748 (2018).
7. Humphrey, P. A., Moch, H., Cubilla, A. L., Ulbright, T. M. & Reuter, V. E. The 2016 WHO Classification of Tumours of the Urinary System and Male Genital Organs—Part B: Prostate and Bladder Tumours. *Eur. Urol.* **70**, 106–119 (2016).
8. Professionals, S.-O. Non-muscle-invasive Bladder Cancer. *Uroweb* Available at: http://uroweb.org/guideline/non-muscle-invasive-bladder-cancer/. (Accessed: 15th July 2018)
9. Lamm, D. *et al.* Defining progression in nonmuscle invasive bladder cancer: it is time for a new, standard definition. *J. Urol.* **191**, 20–27 (2014).
10. Witjes, J. A. *et al.* Updated 2016 EAU Guidelines on Muscle-invasive and Metastatic Bladder Cancer. *Eur. Urol.* **71**, 462–475 (2017).

11. Babjuk, M. *et al.* EAU Guidelines on Non-Muscle-invasive Urothelial Carcinoma of the Bladder: Update 2016. *Eur. Urol.* **71**, 447–461 (2017).

12. Snyder, A. *et al.* Genetic Basis for Clinical Response to CTLA-4 Blockade in Melanoma. *N. Engl. J. Med.* **371**, 2189–2199 (2014).

13. Laumont, C. M. *et al.* Noncoding regions are the main source of targetable tumor-specific antigens. *Sci. Transl. Med.* **10**, eaau5516 (2018).

14. Chodisetti, S. B., Rai, P. K., Gowthaman, U., Pahari, S. & Agrewala, J. N. Potential T cell epitopes of Mycobacterium tuberculosis that can instigate molecular mimicry against host: implications in autoimmune pathogenesis. *BMC Immunol.* **13**, 13 (2012).

15. Zheng, Y. *et al.* Applications of bacillus Calmette-Guerin and recombinant bacillus Calmette-Guerin in vaccine development and tumor immunotherapy. *Expert Rev. Vaccines* **14**, 1255–1275 (2015).

16. Rentsch, C. A. *et al.* Bacillus Calmette-Guérin strain differences have an impact on clinical outcome in bladder cancer immunotherapy. *Eur. Urol.* **66**, 677–688 (2014).

17. Redelman-Sidi, G., Glickman, M. S. & Bochner, B. H. The mechanism of action of BCG therapy for bladder cancer—a current perspective. *Nat. Rev. Urol.* **11**, nrurol.2014.15 (2014).

18. Alvarez-Arguedas, S. *et al.* Therapeutic efficacy of the live-attenuated Mycobacterium tuberculosis vaccine, MTBVAC, in a preclinical model of bladder cancer. *Transl. Res. J. Lab. Clin. Med.* **197**, 32–42 (2018).

19. Ratliff, T. L., Palmer, J. O., McGarr, J. A. & Brown, E. J. Intravesical Bacillus Calmette-Guérin therapy for murine bladder tumors: initiation of the response by

fibronectin-mediated attachment of Bacillus Calmette-Guérin. *Cancer Res.* **47**, 1762–1766 (1987).

20. Mora Vidal, R. *et al.* Epidermal Growth Factor Receptor Family Inhibition Identifies P38 Mitogen-activated Protein Kinase as a Potential Therapeutic Target in Bladder Cancer. *Urology* **112**, 225.e1-225.e7 (2018).
21. Nunez-Nateras, R. *et al.* Predicting response to bacillus Calmette-Guérin (BCG) in patients with carcinoma in situ of the bladder. *Urol. Oncol.* **32**, 45.e23–30 (2014).
22. García-Cuesta, E. M. *et al.* NKG2D is a Key Receptor for Recognition of Bladder Cancer Cells by IL-2-Activated NK Cells and BCG Promotes NK Cell Activation. *Front. Immunol.* **6**, 284 (2015).
23. Hartana, C. A. *et al.* Urothelial bladder cancer may suppress perforin expression in CD8+ T cells by an ICAM-1/TGFβ2 mediated pathway. *PLOS ONE* **13**, e0200079 (2018).
24. Audenet, F. *et al.* Immune phenotype of peripheral blood mononuclear cells in patients with high-risk non-muscle invasive bladder cancer. *World J. Urol.* 1–8 (2018). doi:10.1007/s00345-018-2359-7
25. Romagnani, S. Th1/Th2 cells. *Inflamm. Bowel Dis.* **5**, 285–294 (1999).
26. Saint, F. *et al.* Urinary IL-2 assay for monitoring intravesical bacillus Calmette-Guérin response of superficial bladder cancer during induction course and maintenance therapy. *Int. J. Cancer* **107**, 434–440 (2003).
27. Pichler, R. *et al.* Intratumoral Th2 predisposition combines with an increased Th1 functional phenotype in clinical response to intravesical BCG in bladder cancer. *Cancer Immunol. Immunother.* **66**, 427–440 (2017).

28. Lamm, D. L. *et al.* Maintenance bacillus Calmette-Guerin immunotherapy for recurrent TA, T1 and carcinoma in situ transitional cell carcinoma of the bladder: a randomized Southwest Oncology Group Study. *J. Urol.* **163**, 1124–1129 (2000).

29. Kandeel, W. *et al.* A comparative study between full-dose and half-dose intravesical immune bacille Calmette–Guérin injection in the management of superficial bladder cancer. *Arab J. Urol.* **13**, 233–237 (2015).

30. Martínez-Piñeiro, L. *et al.* Maintenance Therapy with 3-monthly Bacillus Calmette-Guérin for 3 Years is Not Superior to Standard Induction Therapy in High-risk Non–muscle-invasive Urothelial Bladder Carcinoma: Final Results of Randomised CUETO Study 98013. *Eur. Urol.* **68**, 256–262 (2015).

31. LUCA, S. & MIHAESCU, T. History of BCG Vaccine. *Mædica* **8**, 53–58 (2013).

32. Moliva, J. I., Turner, J. & Torrelles, J. B. Immune Responses to Bacillus Calmette–Guérin Vaccination: Why Do They Fail to Protect against Mycobacterium tuberculosis? *Front. Immunol.* **8**, (2017).

33. Martinez, L. *et al.* Transmission of Mycobacterium Tuberculosis in Households and the Community: A Systematic Review and Meta-Analysis. *Am. J. Epidemiol.* **185**, 1327–1339 (2017).

34. Trentini, M. M., de Oliveira, F. M., Kipnis, A. & Junqueira-Kipnis, A. P. The Role of Neutrophils in the Induction of Specific Th1 and Th17 during Vaccination against Tuberculosis. *Front. Microbiol.* **7**, (2016).

35. Yan, Z.-H. *et al.* CD137 is a Useful Marker for Identifying CD4+ T Cell Responses to Mycobacterium tuberculosis. *Scand. J. Immunol.* **85**, 372–380 (2017).

36. Kandoth, C. *et al.* Mutational landscape and significance across 12 major cancer types. *Nature* **502**, 333–339 (2013).

37. Kim, H.-J. & Cantor, H. CD4 T-cell subsets and tumor immunity: the helpful and the not-so-helpful. *Cancer Immunol. Res.* **2**, 91–98 (2014).

38. Azoury, S. C., Straughan, D. M. & Shukla, V. Immune Checkpoint Inhibitors for Cancer Therapy: Clinical Efficacy and Safety. *Curr. Cancer Drug Targets* **15**, 452–462 (2015).

39. Anderson, A. C., Joller, N. & Kuchroo, V. K. Lag-3, Tim-3, and TIGIT co-inhibitory receptors with specialized functions in immune regulation. *Immunity* **44**, 989–1004 (2016).

40. Immunotherapy Drugs Approved for Bladder Cancer. *National Cancer Institute* Available at: https://www.cancer.gov/news-events/cancer-currents-blog/2017/approvals-fda-checkpoint-bladder. (Accessed: 3rd November 2017)

41. Balar, A. V. *et al.* First-line pembrolizumab in cisplatin-ineligible patients with locally advanced and unresectable or metastatic urothelial cancer (KEYNOTE-052): a multicentre, single-arm, phase 2 study. *Lancet Oncol.* **18**, 1483–1492 (2017).

42. Balar, A. V. *et al.* Atezolizumab as first-line therapy in cisplatin-ineligible patients with locally advanced and metastatic urothelial carcinoma: a single-arm, multicentre, phase 2 trial. *Lancet Lond. Engl.* **389**, 67–76 (2017).

43. Albert, S. *et al.* A novel nanobody-based target module for retargeting of T lymphocytes to EGFR-expressing cancer cells via the modular UniCAR platform. *Oncoimmunology* **6**, e1287246 (2017).

44. Cartellieri, M. *et al.* Switching CAR T cells on and off: a novel modular platform for retargeting of T cells to AML blasts. *Blood Cancer J.* **6**, e458 (2016).

45. Arndt, C. *et al.* Costimulation improves the killing capability of T cells redirected to tumor cells expressing low levels of CD33: description of a novel modular targeting system. *Leukemia* **28**, 59–69 (2014).

46. Kamat, A. M. *et al.* BCG-unresponsive non-muscle-invasive bladder cancer: recommendations from the IBCG. *Nat. Rev. Urol.* **14**, 244–255 (2017).

47. Barkan, G. A. *et al.* The Paris System for Reporting Urinary Cytology: The Quest to Develop a Standardized Terminology. *Acta Cytol.* **60**, 185–197 (2016).

48. Gupta, M., VandenBussche, C. J. & Bivalacqua, T. J. Urinary cytology and the Paris system for reporting urinary cytology: Implications for urological management. *Cytopathol. Off. J. Br. Soc. Clin. Cytol.* (2018). doi:10.1111/cyt.12538

49. Kehinde, E. O., Al-Mulla, F., Kapila, K. & Anim, J. T. Comparison of the sensitivity and specificity of urine cytology, urinary nuclear matrix protein-22 and multitarget fluorescence in situ hybridization assay in the detection of bladder cancer. *Scand. J. Urol. Nephrol.* **45**, 113–121 (2011).

50. Zippe, C., Pandrangi, L. & Agarwal, A. NMP22 IS A SENSITIVE, COST-EFFECTIVE TEST IN PATIENTS AT RISK FOR BLADDER CANCER. *J. Urol.* **161**, 62–65 (1999).

51. Hajdinjak, T. UroVysion FISH test for detecting urothelial cancers: Meta-analysis of diagnostic accuracy and comparison with urinary cytology testing. *Urol. Oncol. Semin. Orig. Investig.* **26**, 646–651 (2008).

52. Kamat, A. M. *et al.* Use of Fluorescence in situ Hybridization to Predict Patient Response to BCG Therapy for Bladder Cancer: Results of a Prospective Trial. *J. Urol.* **187**, 862–867 (2012).

53. Jackson, A. M. *et al.* Changes in urinary cytokines and soluble intercellular adhesion molecule-1 (ICAM-1) in bladder cancer patients after bacillus Calmette-Guérin (BCG) immunotherapy. *Clin. Exp. Immunol.* **99**, 369–375 (1995).

54. Kumari, N. *et al.* Predictive role of serum and urinary cytokines in invasion and recurrence of bladder cancer ,
Predictive role of serum and urinary cytokines in invasion and recurrence of bladder cancer. *Tumor Biol.* **39**, 1010428317697552 (2017).

55. Kamat, A. M. *et al.* Cytokine Panel for Response to Intravesical Therapy (CyPRIT): Nomogram of Changes in Urinary Cytokine Levels Predicts Patient Response to Bacillus Calmette-Guérin. *Eur. Urol.* **69**, 197–200 (2016).

56. Rigaud, J. *et al.* Development of Predictive Value of Urinary Cytokine Profile Induced During Intravesical Bacillus Calmette-Guérin Instillations for Bladder Cancer. *Clin. Genitourin. Cancer* **13**, e209–e215 (2015).

57. Kaynar, M. *et al.* Bladder cancer invasion predictability based on preoperative neutrophil–lymphocyte ratio. *Tumor Biol.* **35**, 6601–6605 (2014).

58. Teke, K. *et al.* Monitoring the response of urothelial precancerous lesions to Bacillus Calmette-Guerin at the proteome level in an in vivo rat model. *Cancer Immunol. Immunother. CII* **67**, 67–77 (2018).

59. Rentsch, C. A. *et al.* BCG-Mediated Bladder Cancer Immunotherapy: Identifying Determinants of Treatment Response Using a Calibrated Mathematical Model. *PLOS ONE* **8**, e56327 (2013).

60. Ayub, A., Yale, S. H., Reed, K. D., Nasser, R. M. & Gilbert, S. R. Testing for Latent Tuberculosis. *Clin. Med. Res.* **2**, 191–194 (2004).

61. Muñoz, L. *et al.* QuantiFERON®-TB Gold In-Tube for contact screening in BCG-vaccinated adults: A longitudinal cohort study. *PLoS ONE* **12**, (2017).

62. Seddon, J. A. *et al.* The impact of BCG vaccination on tuberculin skin test responses in children is age dependent: evidence to be considered when screening children for tuberculosis infection. *Thorax* **71**, 932–939 (2016).

63. Lewinsohn, D. M. *et al.* Official American Thoracic Society/Infectious Diseases Society of America/Centers for Disease Control and Prevention Clinical Practice Guidelines: Diagnosis of Tuberculosis in Adults and Children. *Clin. Infect. Dis. Off. Publ. Infect. Dis. Soc. Am.* **64**, 111–115 (2017).

64. Niwa, N. *et al.* MP08-04 PURIFIED PROTEIN DERIVATIVE SKIN TEST PRIOR TO BACILLUS CALMETTE-GUÉRIN THERAPY ENHANCES THE CLINICAL EFFICACY OF BCG THERAPY IN PATIENTS WITH NON-MUSCLE INVASIVE BLADDER CANCER. *J. Urol.* **199**, e97 (2018).

65. Jeong, D. H. *et al.* Comparison of latent tuberculosis infection screening strategies before tumor necrosis factor inhibitor treatment in inflammatory arthritis: IGRA-alone versus combination of TST and IGRA. *PLOS ONE* **13**, e0198756 (2018).

66. Bae, W. *et al.* Comparison of the Sensitivity of QuantiFERON-TB Gold In-Tube and T-SPOT.TB According to Patient Age. *PLoS ONE* **11**, (2016).

67. Barcellini, L. *et al.* First independent evaluation of QuantiFERON-TB Plus performance. *Eur. Respir. J.* **47**, 1587–1590 (2016).

68. Introducing the ESAT-6 free IGRA, a companion diagnostic for TB vaccines based on ESAT-6 | Scientific Reports. Available at: https://www.nature.com/articles/srep45969. (Accessed: 18th July 2018)

69. Wu, J. *et al.* Multiple cytokine responses in discriminating between active tuberculosis and latent tuberculosis infection. *Tuberculosis* **102**, 68–75 (2017).

70. Novel M. tuberculosis specific IL-2 ELISpot assay discriminates adult patients with active or latent tuberculosis. Available at: http://journals.plos.org/plosone/article?id=10.1371/journal.pone.0197825. (Accessed: 18th July 2018)

71. Kim, J. Y. *et al.* Combined IFN-γ and TNF-α release assay for differentiating active tuberculosis from latent tuberculosis infection. *J. Infect.* (2018). doi:10.1016/j.jinf.2018.04.011

72. Musvosvi, M. *et al.* T-cell biomarkers for diagnosis of tuberculosis: candidate evaluation by a simple whole blood assay for clinical translation. *Eur. Respir. J.* **51**, (2018).

73. Bacher, P. & Scheffold, A. Flow-cytometric analysis of rare antigen-specific T cells. *Cytometry A* **83A**, 692–701 (2013).

74. Elsäßer, J. *et al.* Antigen-Specific CD4 T Cells Are Induced after Intravesical BCG-Instillation Therapy in Patients with Bladder Cancer and Show Similar Cytokine Profiles as in Active Tuberculosis. *PLoS ONE* **8**, (2013).

75. Cohen, C. J. *et al.* Isolation of neoantigen-specific T cells from tumor and peripheral lymphocytes. *J. Clin. Invest.* **125**, 3981–3991 (2015).

76. Shen, C. *et al.* Frequency and reactivity of antigen-specific T cells were concurrently measured through the combination of artificial antigen-presenting cell, MACS and ELISPOT. *Sci. Rep.* **7**, 16400 (2017).

77. Hou, H. *et al.* Establishment of the Reference Intervals of Lymphocyte Function in Healthy Adults Based on IFN-γ Secretion Assay upon Phorbol-12-Myristate-13-Acetate/Ionomycin Stimulation. *Front. Immunol.* **9**, (2018).

78. Meilleur, C. E. *et al.* Bacterial Superantigens Expand and Activate, Rather than Delete or Incapacitate, Preexisting Antigen-Specific Memory TCD8. *J. Infect. Dis.* doi:10.1093/infdis/jiy647

79. PROFT, T. & FRASER, J. D. Bacterial superantigens. *Clin. Exp. Immunol.* **133**, 299–306 (2003).

80. Langley, R. J. *et al.* Staphylococcal enterotoxin-like X (SElX) is a unique superantigen with functional features of two major families of staphylococcal virulence factors. *PLOS Pathog.* **13**, e1006549 (2017).

81. Li, Z. *et al.* Staphylococcal Superantigens Use LAMA2 as a Coreceptor To Activate T Cells. *J. Immunol.* ji1701212 (2018). doi:10.4049/jimmunol.1701212

82. Xie, Y. *et al.* In vitro effects of Staphylococcus aureus enterotoxin C3 on T cell activation, proliferation and cytokine production. *Mol. Med. Rep.* **16**, 4744–4750 (2017).

83. Leder, L. *et al.* A Mutational Analysis of the Binding of Staphylococcal Enterotoxins B and C3 to the T Cell Receptor β Chain and Major Histocompatibility Complex Class II. *J. Exp. Med.* **187**, 823–833 (1998).

84. Klenerman, P. & Oxenius, A. T cell responses to cytomegalovirus. *Nat. Rev. Immunol.* **16**, 367–377 (2016).

85. Sylwester, A. W. *et al.* Broadly targeted human cytomegalovirus-specific CD4+ and CD8+ T cells dominate the memory compartments of exposed subjects. *J. Exp. Med.* **202**, 673–685 (2005).

86. Quinn, M., Erkes, D. A. & Snyder, C. M. Cytomegalovirus and immunotherapy: opportunistic pathogen, novel target for cancer and a promising vaccine vector. *Immunotherapy* **8**, 211–221 (2016).

87. Sester, U. *et al.* Whole-Blood Flow-Cytometric Analysis of Antigen-Specific CD4 T-Cell Cytokine Profiles Distinguishes Active Tuberculosis from Non-Active States. *PLoS ONE* **6**, (2011).

88. Mahnke, Y. D. & Roederer, M. OMIP-001: Quality and phenotype of Ag-responsive human T-cells. *Cytometry A* **77A**, 819–820 (2010).

89. Lamoreaux, L., Koup, R. A. & Roederer, M. OMIP-009: Characterization of antigen-specific human T-cells. *Cytom. Part J. Int. Soc. Anal. Cytol.* **81**, 362–363 (2012).

90. De Rosa, S. C., Carter, D. K. & McElrath, M. J. OMIP-014: validated multifunctional characterization of antigen-specific human T cells by intracellular cytokine staining. *Cytom. Part J. Int. Soc. Anal. Cytol.* **81**, 1019–1021 (2012).

91. Graves, A. J., Padilla, M. G. & Hokey, D. A. OMIP-022: Comprehensive assessment of antigen-specific human T-cell functionality and memory. *Cytometry* **85**, 576–579 (2014).

92. Bocsi, J., Melzer, S., Dähnert, I. & Tárnok, A. OMIP-023: 10-Color, 13 antibody panel for in-depth phenotyping of human peripheral blood leukocytes. *Cytometry A* **85**, 781–784 (2014).

93. Belkina, A. C. & Snyder-Cappione, J. E. OMIP-037: 16-color panel to measure inhibitory receptor signatures from multiple human immune cell subsets. *Cytometry A* **91**, 175–179 (2017).

94. Lichtenstein, L. M. & Osler, A. G. STUDIES ON THE MECHANISMS OF HYPERSENSITIVITY PHENOMENA. IX. HISTAMINE RELEASE FROM HUMAN LEUKOCYTES BY RAGWEED POLLEN ANTIGEN. *J. Exp. Med.* **120**, 507–530 (1964).

95. Yun, S.-H., Sim, E.-H., Goh, R.-Y., Park, J.-I. & Han, J.-Y. Platelet Activation: The Mechanisms and Potential Biomarkers. *BioMed Res. Int.* **2016**, (2016).

96. Blair, T. A., Michelson, A. D. & Frelinger, A. L. Mass Cytometry Reveals Distinct Platelet Subtypes in Healthy Subjects and Novel Alterations in Surface Glycoproteins in Glanzmann Thrombasthenia. *Sci. Rep.* **8**, (2018).

97. Hancharou, A., Ramanava, I. & Dubuske, L. Novel Basophil Activation and Degranulation Markers for the Basophil Activation Test. *J. Allergy Clin. Immunol.* **141**, AB228 (2018).

98. Ornelas, C. *et al.* The Contribution of the Basophil Activation Test to the Diagnosis of Hypersensitivity Reactions to Oxaliplatin. *Int. Arch. Allergy Immunol.* 1–7 (2018). doi:10.1159/000490313

99. MacGlashan, D. Expression of CD203c and CD63 in Human Basophils: Relationship to Differential Regulation of Piecemeal and Anaphylactic Degranulation Processes. *Clin. Exp. Allergy J. Br. Soc. Allergy Clin. Immunol.* **40**, 1365–1377 (2010).

100. Amano, T., Furuno, T., Hirashima, N., Ohyama, N. & Nakanishi, M. Dynamics of Intracellular Granules with CD63-GFP in Rat Basophilic Leukemia Cells. *J. Biochem. (Tokyo)* **129**, 739–744 (2001).

101. Betts, M. R. & Koup, R. A. Detection of T-cell degranulation: CD107a and b. *Methods Cell Biol.* **75**, 497–512 (2004).

102. Aktas, E., Kucuksezer, U. C., Bilgic, S., Erten, G. & Deniz, G. Relationship between CD107a expression and cytotoxic activity. *Cell. Immunol.* **254**, 149–154 (2009).

103. van Velzen, J. F., Laros-van Gorkom, B. A. P., Pop, G. A. M. & van Heerde, W. L. Multicolor flow cytometry for evaluation of platelet surface antigens and activation markers. *Thromb. Res.* **130**, 92–98 (2012).

104. Stuehler, C. *et al.* Multispecific Aspergillus T Cells Selected by CD137 or CD154 Induce Protective Immune Responses Against the Most Relevant Mold Infections. *J. Infect. Dis.* **211**, 1251–1261 (2015).

105. Cooper, D., Bansal-Pakala, P. & Croft, M. 4-1BB (CD137) controls the clonal expansion and survival of CD8 T cells in vivo but does not contribute to the development of cytotoxicity. *Eur. J. Immunol.* **32**, 521–529 (2002).

106. Ye, Q. *et al.* CD137 accurately identifies and enriches for naturally-occurring tumor-reactive T cells in tumor. *Clin. Cancer Res. Off. J. Am. Assoc. Cancer Res.* **20**, 44–55 (2014).

107. Litjens, N. H. R., de Wit, E. A., Baan, C. C. & Betjes, M. G. H. Activation-induced CD137 is a fast assay for identification and multi-parameter flow cytometric analysis of alloreactive T cells. *Clin. Exp. Immunol.* **174**, 179–191 (2013).

108. Ye, Q. *et al.* CD137 accurately identifies and enriches for naturally occurring tumor-reactive T cells in tumor. *Clin. Cancer Res. Off. J. Am. Assoc. Cancer Res.* **20**, 44–55 (2014).

109. Wölfl, M., Kuball, J., Eyrich, M., Schlegel, P. G. & Greenberg, P. D. Use of CD137 to study the full repertoire of CD8+ T cells without the need to know epitope specificities. *Cytom. Part J. Int. Soc. Anal. Cytol.* **73**, 1043–1049 (2008).

110. Blotta, M. H., Marshall, J. D., DeKruyff, R. H. & Umetsu, D. T. Cross-linking of the CD40 ligand on human CD4+ T lymphocytes generates a costimulatory signal that up-regulates IL-4 synthesis. *J. Immunol.* **156**, 3133–3140 (1996).

111. Mikolajczak, S. A. *et al.* The modulation of CD40 ligand signaling by transmembrane CD28 splice variant in human T cells. *J. Exp. Med.* **199**, 1025–1031 (2004).

112. Möller, J. F., Möller, B., Wiedenmann, B., Berg, T. & Schott, E. CD154, a marker of antigen-specific stimulation of CD4 T cells, is associated with response to treatment in patients with chronic HCV infection. *J. Viral Hepat.* **18**, e341-349 (2011).

113. Pera, A. *et al.* CMV induces expansion of highly polyfunctional CD4+ T cell subset coexpressing CD57 and CD154. *J. Leukoc. Biol.* **101**, 555–566 (2017).

114. Shan, G., Tang, T., Qian, H. & Xia, Y. Certain BCG-reactive responses are associated with bladder cancer prognosis. *Cancer Immunol. Immunother. CII* **67**, 797–803 (2018).

115. Zorn, E. *et al.* IL-2 regulates FOXP3 expression in human CD4+CD25+ regulatory T cells through a STAT-dependent mechanism and induces the expansion of these cells in vivo. *Blood* **108**, 1571–1579 (2006).

116. Cho, J.-H. *et al.* Unique Features of Naive CD8+ T Cell Activation by IL-2. *J. Immunol.* **191**, 5559–5573 (2013).

117. Schoenborn, J. R. & Wilson, C. B. Regulation of Interferon- γ During Innate and Adaptive Immune Responses. in *Advances in Immunology* **96**, 41–101 (Academic Press, 2007).

118. Ouchi, N. *et al.* Adiponectin, an adipocyte-derived plasma protein, inhibits endothelial NF-kappaB signaling through a cAMP-dependent pathway. *Circulation* **102**, 1296–1301 (2000).

119. Shikotra, A., Ohri, C. M., Green, R. H., Waller, D. A. & Bradding, P. Mast cell phenotype, TNFα expression and degranulation status in non-small cell lung cancer. *Sci. Rep.* **6**, (2016).

120. Bertrand, F. *et al.* Blocking Tumor Necrosis Factor α Enhances CD8 T-cell–Dependent Immunity in Experimental Melanoma. *Cancer Res.* **75**, 2619–2628 (2015).

121. Bauswein, M. *et al.* Human T cells modulate myeloid-derived suppressor cells through a TNF-α-mediated mechanism. *Immunol. Lett.* (2018). doi:10.1016/j.imlet.2018.07.010

122. Blair, T. A., Michelson, A. D. & Frelinger, A. L. Mass Cytometry Reveals Distinct Platelet Subtypes in Healthy Subjects and Novel Alterations in Surface Glycoproteins in Glanzmann Thrombasthenia. *Sci. Rep.* **8**, 10300 (2018).

123. Brecher, G., Schneiderman, M. & Cronkite, E. P. The reproducibility and constancy of the platelet count. *Am. J. Clin. Pathol.* **23**, 15–26 (1953).

124. Blair, T. A., Michelson, A. D. & Frelinger, A. L. Mass Cytometry Reveals Distinct Platelet Subtypes in Healthy Subjects and Novel Alterations in Surface Glycoproteins in Glanzmann Thrombasthenia. *Sci. Rep.* **8**, 10300 (2018).

125. Chevrier, S. *et al.* Compensation of Signal Spillover in Suspension and Imaging Mass Cytometry. *Cell Syst.* **6**, 612-620.e5 (2018).

126. Jimenez-Carretero, D., Ligos, J. M., Martínez-López, M., Sancho, D. & Montoya, M. C. Flow Cytometry Data Preparation Guidelines for Improved Automated Phenotypic Analysis. *J. Immunol.* **200**, 3319–3331 (2018).

127. Jansen, J. J. *et al.* FLOOD: FLow cytometric Orthogonal Orientation for Diagnosis. *Chemom. Intell. Lab. Syst.* **151**, 126–135 (2016).

128. Kaighn, M. E., Narayan, K. S., Ohnuki, Y., Lechner, J. F. & Jones, L. W. Establishment and characterization of a human prostatic carcinoma cell line (PC-3). *Invest. Urol.* **17**, 16–23 (1979).

129. Horoszewicz, J. S. *et al.* The LNCaP cell line--a new model for studies on human prostatic carcinoma. *Prog. Clin. Biol. Res.* **37**, 115–132 (1980).

130. Chang, S., Kohrt, H. & Maecker, H. T. Monitoring the Immune Competence of Cancer Patients to Predict Outcome. *Cancer Immunol. Immunother. CII* **63**, 713–719 (2014).

131. Bosire, E. M. *et al.* Population specific reference ranges of CD3, CD4 and CD8 lymphocyte subsets among healthy Kenyans. *AIDS Res. Ther.* **10**, 24 (2013).

132. Baran, J., Kowalczyk, D., Oz˙óg, M. & Zembala, M. Three-Color Flow Cytometry Detection of Intracellular Cytokines in Peripheral Blood Mononuclear Cells: Comparative Analysis of Phorbol Myristate Acetate-Ionomycin and Phytohemagglutinin Stimulation. *Clin. Diagn. Lab. Immunol.* **8**, 303–313 (2001).

133. Saxena, A., Dagur, P. K., Desai, A. & McCoy, J. P. Ultrasensitive Quantification of Cytokine Proteins in Single Lymphocytes From Human Blood Following ex-vivo Stimulation. *Front. Immunol.* **9**, (2018).

134. Kraft, S. *et al.* The tetraspanin CD63 is required for efficient IgE-mediated mast cell degranulation and anaphylaxis. *J. Immunol. Baltim. Md 1950* **191**, 2871–2878 (2013).

135. Betts, M. R. *et al.* Sensitive and viable identification of antigen-specific CD8+ T cells by a flow cytometric assay for degranulation. *J. Immunol. Methods* **281**, 65–78 (2003).

136. O'Neil-Andersen, N. J. & Lawrence, D. A. Differential Modulation of Surface and Intracellular Protein Expression by T Cells after Stimulation in the Presence of Monensin or Brefeldin A. *Clin. Diagn. Lab. Immunol.* **9**, 243–250 (2002).

137. Simms, P. E. & Ellis, T. M. Utility of flow cytometric detection of CD69 expression as a rapid method for determining poly- and oligoclonal lymphocyte activation. *Clin. Diagn. Lab. Immunol.* **3**, 301–304 (1996).

138. Nakaima, Y., Watanabe, K., Koyama, T., Miura, O. & Fukuda, T. CD137 Is Induced by the CD40 Signal on Chronic Lymphocytic Leukemia B Cells and Transduces the Survival Signal via NF-κB Activation. *PLoS ONE* **8**, (2013).

139. Ai, W., Li, H., Song, N., Li, L. & Chen, H. Optimal Method to Stimulate Cytokine Production and Its Use in Immunotoxicity Assessment. *Int. J. Environ. Res. Public. Health* **10**, 3834–3842 (2013).

140. Jung, T., Schauer, U., Heusser, C., Neumann, C. & Rieger, C. Detection of intracellular cytokines by flow cytometry. *J. Immunol. Methods* **159**, 197–207 (1993).

141. van der Heiden, P. L. J. *et al.* CMV seronegative donors: Effect on clinical severity of CMV infection and reconstitution of CMV-specific immunity. *Transpl. Immunol.* **49**, 54–58 (2018).

142. Cho, J. H., Collins, J. J. & Wong, W. W. Universal Chimeric Antigen Receptors for Multiplexed and Logical Control of T Cell Responses. *Cell* **173**, 1426-1438.e11 (2018).